



An efficient spline method to solve two-parameter 1D parabolic singularly perturbed systems with time delay and different diffusion parameters

Parvin Kumari¹ · Carmelo Clavero²

Received: 3 September 2025 / Revised: 14 October 2025 / Accepted: 17 October 2025
© The Author(s) 2025

Abstract

In this paper, we are interested in the efficient numerical resolution of one dimensional two-parameter singularly perturbed systems; for simplicity, we only give the theoretically details corresponding to the simplest case of systems with two equations. The diffusion parameters are distinct and can have a very different value; on the other hand, the convection parameter is the same for both equations. Finally, we assume that a large time delays term appears in the partial differential equation. So, the exact solution has overlapping boundary layers at both end points of the spatial interval, when the magnitude of the diffusion parameters is very different; the behavior of the boundary layers depends on the value and the ratio between the diffusion and the convection parameters. To approximate the exact solution of the continuous problem, we construct a numerical method, which combines the Crank-Nicolson method to discretize in time, which is constructed on a uniform mesh, and a type of B -splines to discretize in space, which are defined on a special nonuniform Shishkin mesh. We prove that the fully discrete scheme is a uniformly convergent method, having second order in time and almost second order in space. From a practical point of view, higher order numerical methods are convenient because they permit to obtain good numerical approximations with a small increase of the computational cost. To corroborate in practice the good properties of the numerical method, some test problems are solved; from the numerical results obtained for these examples, clearly follows both the efficiency and the order of uniform convergence of the numerical method, in agreement with the theoretical results.

Keywords Singularly perturbed systems · Small different diffusion parameters · Small equal convection parameters · Shishkin meshes · Spline methods · High-order accuracy

Extended author information available on the last page of the article

2010 MSC 35B25 · 35B50 · 35K51 · 35K57 · 65L70 · 65M12 · 65M15 · 65M22 · 65M50

1 Introduction

In this work, we solve 1D systems of singularly perturbed delay parabolic IBVP on $\mathcal{M} = \mathcal{M}_x \times \mathcal{M}_s = (0, 1) \times (0, S]$, which are defined by

$$\mathcal{L}\mathbf{X} := \frac{\partial \mathbf{X}}{\partial s} + \mathcal{L}_{x, \varepsilon_1, \varepsilon_2, \nu} \mathbf{X} = -a(x)\mathbf{X}(x, s - \tau) + \mathbf{f}(x, s), \quad (x, s) \in \mathcal{M}, \quad (1.1a)$$

$$X(0, s) = \varphi_l(s) \text{ in } \mathcal{M}_l, \quad \mathbf{X}(1, s) = \varphi_r(s) \text{ in } \mathcal{M}_r, \quad \mathbf{X}(x, s) = \psi(x, s) \text{ in } \mathcal{M}_b, \quad (1.1b)$$

where

$\mathcal{M}_l = \{(0, s) \mid 0 \leq s \leq S\}$, $\mathcal{M}_r = \{(1, s) \mid 0 \leq s \leq S\}$, $\mathcal{M}_b = \overline{\mathcal{M}}_x \times \Lambda^* = [0, 1] \times (-\tau, 0]$, $\tau > 0$ is a constant and $\mathcal{L} = (\mathcal{L}_1, \mathcal{L}_2)^T$. Without loss of generality, we assume that $0 < \varepsilon_1 \leq \varepsilon_2 \leq 1$ and $0 \leq \nu \leq 1$. Further, the operators $\mathcal{L}_{x, \varepsilon_1, \varepsilon_2, \nu}$ and \mathcal{L}_k , $k = 1, 2$, are defined as

$$\begin{aligned} \mathcal{L}_{x, \varepsilon_1, \varepsilon_2, \nu} &= -E_1 \frac{\partial^2}{\partial x^2} - E_2 P(x) \frac{\partial}{\partial x} + Q(x, s), \\ \mathcal{L}_k \mathbf{X} &= \frac{\partial X_k}{\partial s} - \varepsilon_k \frac{\partial^2 X_k}{\partial x^2} - \nu p_{kk}(x) \frac{\partial X_k}{\partial x} + \sum_{j=1}^2 q_{kj}(x, s) X_j, \quad k = 1, 2, \end{aligned}$$

$$\text{where } E_1 = \begin{pmatrix} \varepsilon_1 & 0 \\ 0 & \varepsilon_2 \end{pmatrix}, E_2 = \begin{pmatrix} \nu & 0 \\ 0 & \nu \end{pmatrix}, P(x) = \begin{pmatrix} p_{11}(x) & 0 \\ 0 & p_{22}(x) \end{pmatrix},$$

$$Q(x, s) = \begin{pmatrix} q_{11}(x, s) & q_{12}(x, s) \\ q_{21}(x, s) & q_{22}(x, s) \end{pmatrix},$$

$\mathbf{f}(x, s) = (f_1(x, s), f_2(x, s))^T$, $\mathbf{X}(x, s) = (X_1(x, s), X_2(x, s))^T$, $\varphi_l(s) = (\varphi_{l_1}(s), \varphi_{l_2}(s))^T$, $\varphi_r(s) = (\varphi_{r_1}(s), \varphi_{r_2}(s))^T$. For each $(x, s) \in \overline{\mathcal{M}}$ and $x \in \mathcal{M}_x$, the coefficients of matrices $P(x)$ and $Q(x, s)$ satisfy

$$p_{kk}(x) \geq \alpha_k > 0, \quad k = 1, 2, \quad (1.2a)$$

$$Q(x, s) \text{ is an } L_0 \text{ matrix} \Rightarrow q_{kj}(x, s) \leq 0, \quad k \neq j, \quad q_{kk} > 0, \quad k, j = 1, 2, \quad (1.2b)$$

$$\sum_{j=1}^2 q_{kj}(x, s) \geq \Phi > 0, \quad q_{kk}(x, s) > |q_{kj}(x, s)|, \quad k, j = 1, 2, \quad k \neq j. \quad (1.2c)$$

Below, we denote by $\alpha = \min\{\alpha_1, \alpha_2\}$,

$$\eta = \min_{(x,s) \in \bar{\mathcal{M}}} \left\{ \frac{q_{k1}(x, s) - q_{k2}(x, s)}{p_{kk}(x)} \right\}, \quad k = 1, 2, \vec{\varepsilon} = (\varepsilon_1, \varepsilon_2)^T \text{ and } \vec{\nu} = (\nu, \nu)^T.$$

From a practical point of view, this type of systems is interesting because they are a good model in many applications' areas, such as chemical reactor dynamics, brain signal transmission, climate modelling, power system stability or epidemiology (see, for instance, [11, 19, 20, 22, 25]). In all these applications, the solution of the physical phenomena has a multi-scale behavior due the presence of small diffusion and convection parameters; moreover, the effects of temporal delays are caused by different characteristic as transport lags, feedback control loops or incubation periods, depending on the particular problem. It is well known that, in general, the presence of time delay and small perturbation parameters in both the diffusion and the convection terms, provokes that the solution has a very different behavior and very large step gradients on different regions in the domain. The main characteristic of these systems is the presence of positive parameters multiplying both the first and the second spatial partial derivatives. Moreover, large time delays, such as the average process time of a control loop, can cause boundary layers, oscillations and a negative impact on the system's stability of the numerical method used to solve the continuous problem.

In many physical, chemical and biological systems, the evolution of multiple interacting species is governed by convection-reaction-diffusion mechanisms. The interaction of slowly diffusing morphogens and faster-moving proteins drives the establishment of spatial patterns in gene regulatory networks, where transcriptional and translational delays cause past morphogen concentrations to control protein synthesis. To analyze such processes, we consider a coupled system of convection-reaction-diffusion equations with unequal diffusion parameters and a large time delay, which captures the essential features of delayed feedback and multiscale spatial transport. An example framework for studying these effects in a physiologically relevant context is provided by the model that follows.

1.1 Motivating model: convection-reaction-diffusion system in gene regulatory networks

This system can be modeled as a set of coupled singularly perturbed convection-reaction-diffusion equations with different diffusion parameters and a large time delay, given by

$$\frac{\partial X_1}{\partial s} = \epsilon_1 \frac{\partial^2 X_1}{\partial x^2} - \nu b_1(x) \frac{\partial X_1}{\partial x} - a_1(x) X_1 + f_1(X_1, X_2), \quad (1.3)$$

$$\frac{\partial X_2}{\partial s} = \epsilon_2 \frac{\partial^2 X_2}{\partial x^2} - \nu b_2(x) \frac{\partial X_2}{\partial x} - a_2(x) X_2 + f_2(X_1(x, s - \tau), X_2), \quad (1.4)$$

subject to the boundary and initial conditions

$$\begin{aligned} X_1(0, s) &= X_1(1, s) = 0, & X_2(0, s) &= X_2(1, s) = 0, & s \in [0, S], \\ X_1(x, s) &= \phi_1(x, s), & X_2(x, s) &= \phi_2(x, s), & s \in [-\tau, 0], x \in (0, 1). \end{aligned}$$

In this case, $X_1(x, s)$ and $X_2(x, s)$ represent the morphogen and protein concentrations, respectively. The diffusion coefficients of the morphogen and protein are represented by the small positive parameters $\epsilon_1 \ll \epsilon_2$. Moreover, f_1 and f_2 are nonlinear reaction terms that approximate the morphogen auto-regulation and protein synthesis, the functions $a_1(x)$ and $a_2(x)$ indicate spatially changing degradation rates. The term $X_1(x, s - \tau)$ introduces a delay $\tau > 0$ that accounts for the biological time-lag in protein synthesis after the morphogen signal is detected. This delay is considered *large* in the sense that τ is comparable to or greater than the characteristic reaction/diffusion timescale.

Important features of morphogen-controlled gene regulatory networks (GRNs) throughout development are captured by the model. The system's key features are:

- **Different diffusion rates:** $\epsilon_1 \neq \epsilon_2$ models the realistic scenario where morphogens (large molecules) diffuse slowly compared to proteins, which can be transported more rapidly across tissues.
- **Large delay:** The delay τ reflects the temporal gap due to the sequential processes of transcription and translation in protein production.
- **Spatio-temporal patterns:** The interplay between differential diffusion and delay can lead to complex spatial patterns and temporal oscillations, which are fundamental in biological pattern formation (e.g., stripes, spots).

Such models play a crucial role in elucidating developmental patterning mechanisms and serve as valuable benchmarks for testing advanced numerical schemes.

Due to its broad relevance in control systems, chemical kinetics, population dynamics and other real-world processes requiring time delays and small perturbation parameters, the numerical analysis of singularly perturbed delay differential equations (SPDDEs) has attracted a lot of attention. These issues are distinguished by the existence of interior or boundary layers, which makes numerical approximation very difficult. The development of parameter-uniform methods is necessary because traditional numerical approaches frequently fall short in accurately capturing the rapid variations when the perturbation parameter is small. Several researchers have proposed robust numerical techniques to address these issues, including fitted operator schemes, layer-adapted meshes and spline-based collocation approaches. Bansal and Sharma [3] developed a parameter-robust numerical scheme for time-dependent singularly perturbed reaction-diffusion problems with large delay. Sharma and Sharma [28] analyzed a fitted mesh method for delay singularly perturbed systems and Miller, O'Riordan and Shishkin [23] provided a comprehensive theoretical framework for parameter-uniform numerical methods. Furthermore, Kadlabajoo and Patidar [14] discussed numerical techniques for delay differential equations with singular perturbations, while Mohanty and Jha [24] proposed a cubic spline collocation approach for singularly perturbed time-delay systems. Such studies highlight the ongoing efforts to construct efficient and uniformly convergent algorithms capable of resolving the sharp boundary and interior layers present in SPDDEs.

The efficient numerical resolution of elliptic or parabolic coupled singularly perturbed systems in the cases of one or two dimensional problems in space, is a interesting subject in the context of singularly perturbed problems, which has received many attention in the last years. For instance, in [1], a semilinear parabolic problem

was analyzed; in [2], a finite element method was used to solve a singularly perturbed problem with two parameter; in [4], it was used a numerical method combining a finite differences scheme together with the Successive Complementary Expansion Method (SCEM); in [15], a fitted mesh B-spline collocation was employed to solve a singularly perturbed differential-difference equations with large delays; in [31], a numerical technique was used for a type of singularly perturbed parabolic time delay convection-diffusion-reaction equations; in [17], a one dimensional efficient numerical method was introduced for singularly perturbed time-delayed parabolic problems with two parameters; in [19], a time-dependent singularly perturbed system with small shifts was solved, by using first the standard Taylor expansions to transform the original problem and solving the resulting problem by using the Crank-Nicolson method to discretize in time and a cubic B-spline collocation method, constructed on an appropriated Shishkin mesh; in [7], a nonlinear singularly perturbed systems was studied; the numerical scheme defined in that work combines an implicit method to discretize in time, which uses a suitable component splitting, with a finite differences scheme; in [8], a 2D elliptic singularly perturbed system was considered, having the same diffusion parameters and also the same convection parameters in the equations of the system; in [9], a similar technique was used for the case when the diffusion parameters can be different and in [10] for the most general case for which both the diffusion and the convection parameters can be all different; in [20], a similar problem to (1.1) for the simpler case when the diffusion parameters are the same, was studied.

Here, we extend the ideas and techniques given in [20] to our most general and difficult problem (1.1). The presence of distinct diffusion parameters at each equation of the system, does more difficult the theoretical analysis of the asymptotic behavior of the exact solution, because now, when those diffusion parameters has a different order of magnitude, overlapping boundary layers can appear in the solution. Nevertheless, we will prove that using again the Crank-Nicolson method to discretize in time, on a uniform mesh, and a cubic spline-based method to discretize in space, on an adequate piecewise uniform Shishkin mesh, we obtain a high order uniformly convergent method, which is very efficient to solve numerically problem (1.1).

The paper is structured as follows. In Section 2, we analyze which is the asymptotic behavior of the exact solution of the continuous problem and we prove adequate estimates for its partial derivatives, which show their dependence on the diffusion parameters $\varepsilon_1, \varepsilon_2$ and the convection parameter ν ; more concretely, we will distinguish several cases depending on the value and the ratio between those three small parameters. In Sect. 3, we construct the fully discrete scheme into two steps; in the first one, we discretize in time on a uniform mesh and in the second one, we discretize in space on an adequate piecewise uniform Shishkin mesh. In Sect. 4, we prove that the fully discrete scheme is a uniformly convergent method, which gives second order in time and almost second order in space. In Sect. 5, we show the numerical results obtained by using our numerical algorithm for some test problems; from them, we can observe both the efficiency and the uniform convergence of the numerical algorithm, in agreement with the theoretical results. To finish, in Sect. 6, some conclusions are given.

Henceforth, we denote by $\|\cdot\|$ the continuous maximum norm; moreover, for a function $\vec{\Psi} = (\Psi_1, \Psi_2)^T$, $|\vec{\Psi}| = (|\Psi_1|, |\Psi_2|)^T$, and C denotes a generic positive constant which is independent of the diffusion parameters $\varepsilon_1, \varepsilon_2$, the convection parameter ν and also of the discretization parameters N_s and N_x .

2 Asymptotic behavior of the exact solution

In this section, we study which is the asymptotic behavior of the exact solution of (1.1) and we prove adequate estimates for its partial derivatives, which will be useful in the posterior analysis of the uniform convergence of the proposed numerical method.

Using standard techniques, well known in the literature (see [6, 12, 19, 26, 29], for instance), we can obtain the following results, proving that the differential operator \mathcal{L} satisfies a maximum principle and the stability for the continuous function \mathbf{X} , respectively.

Lemma 2.1 Let $\mathbf{X} \in (C^{(2,1)}(\mathcal{M}) \cap C^{(0,0)}(\overline{\mathcal{M}}))^2$ so that $\mathbf{X} \geq \mathbf{0}$ on Λ ($\Lambda = \mathcal{M}_l \cup \mathcal{M}_r \cup \mathcal{M}_b$). Then $\mathcal{L}\mathbf{X} \geq \mathbf{0}$, for all $(x, s) \in \mathcal{M}$ provides $\mathbf{X} \geq \mathbf{0}$, $\forall (x, s) \in \overline{\mathcal{M}}$.

Lemma 2.2 Let \mathbf{X} be the exact solution of the continuous problem (1.1); then, it holds

$$\|\mathbf{X}\|_{\overline{\mathcal{M}}} \leq \frac{1}{\alpha} \|\mathbf{f}\|_{\overline{\mathcal{M}}} + \max\{\|\varphi_l(s)\|_{\overline{\mathcal{M}}_s}, \|\varphi_r(s)\|_{\overline{\mathcal{M}}_s}\}.$$

Following to [21] we can obtain initial estimates for the partial derivatives of the exact solution which depend on both the diffusion and the convection parameters.

Lemma 2.3 Let \mathbf{X} be the exact solution of the continuous problem (1.1). Then, for $l, m = 0, 1, 2, 3, 4$ with $0 \leq 2l + m \leq 4$, its derivatives, on \mathcal{M} , satisfy

$$\left| \frac{\partial^{l+m} \mathbf{X}}{\partial s^l \partial x^m} \right| \leq C(\vec{\varepsilon})^{-m/2} \left\{ 1 + \left(\frac{\vec{\nu}}{\sqrt{\vec{\varepsilon}}} \right)^m \right\}, \quad (2.1a)$$

$$\left| \frac{\partial^{l+m} X_1}{\partial s^l \partial x^m} \right| \leq C \varepsilon_1^{-m/2} \left\{ 1 + \left(\frac{\nu}{\sqrt{\varepsilon_1}} \right)^m \right\} + C \varepsilon_1^{2-m}, \quad (2.1b)$$

$$\left| \frac{\partial^{l+m} X_2}{\partial s^l \partial x^m} \right| \leq C \varepsilon_2^{-m/2} \left\{ 1 + \left(\frac{\nu}{\sqrt{\varepsilon_2}} \right)^m \right\} + C \varepsilon_1^{1-m/2} \varepsilon_2^{-1}. \quad (2.1c)$$

Nevertheless, the estimates given in Lemma 2.3 are not adequate, because they do not reflect the presence of boundary layers in the exact solution of the continuous problem. To obtain better estimates, as it is usual in the context of singularly per-

turbed problems, we propose a decomposition of the exact solution \mathbf{X} of the problem (1.1), in its regular, \mathbf{X}_r , left, \mathbf{X}_L , and right, \mathbf{X}_R , singular components, in the form $\mathbf{X} = \mathbf{X}_r + \mathbf{X}_L + \mathbf{X}_R$. These components are the solution of the problems

$$\begin{cases} \mathcal{L}\mathbf{X}_r = \mathbf{f}(x, s), \quad \mathbf{X}_r(x, 0), \quad \mathbf{X}_r(x, 1) \text{ chosen suitably,} \quad \mathbf{X}_r(x, s)|_{\mathcal{M}_b} = \psi(x, s), \\ \mathcal{L}\mathbf{X}_L = \mathbf{0}, \quad \mathbf{X}_L|_{\mathcal{M}_l} = \mathbf{X} - \mathbf{X}_r - \mathbf{X}_R, \quad \mathbf{X}_L|_{\mathcal{M}_r} \text{ chosen suitably,} \quad \mathbf{X}_L(x, s)|_{\mathcal{M}_b} = \mathbf{0}, \\ \mathcal{L}\mathbf{X}_R = \mathbf{0}, \quad \mathbf{X}_R|_{\mathcal{M}_r} = \mathbf{X} - \mathbf{X}_r - \mathbf{X}_L, \quad \mathbf{X}_R|_{\mathcal{M}_l} \text{ chosen suitably,} \quad \mathbf{X}_R(x, s)|_{\mathcal{M}_b} = \mathbf{0}, \end{cases} \quad (2.2)$$

respectively.

To obtain adequate bounds for the partial derivatives of each one of these three components, we distinguish three different cases depending on the value and the ratio between the diffusion and the convection parameters; these cases are the following: **Case I:** $\alpha \nu^2 \leq \eta \varepsilon_1$; **Case II:** $\alpha \nu^2 \geq \eta \varepsilon_2$; **Case III:** $\eta \varepsilon_1 < \alpha \nu^2 < \eta \varepsilon_2$

Following similar ideas of those ones used in [20], we can deduce adequate estimates for the regular and the singular components, \mathbf{X}_r , \mathbf{X}_L and \mathbf{X}_R , respectively. First, we show the result for the regular component.

Lemma 2.4 *Let $0 \leq 2l + m \leq 4$ be; then, the regular component \mathbf{X}_r satisfy the following bounds.*

Case I: $\alpha \nu^2 \leq \eta \varepsilon_1$. Then, we have

$$\begin{aligned} \left\| \frac{\partial^{l+m} \mathbf{X}_{r1}(x, t)}{\partial s^l \partial x^m} \right\| &\leq C, \quad 0 \leq m \leq 2, \quad \left\| \frac{\partial^{l+m} \mathbf{X}_{r1}(x, t)}{\partial s^l \partial x^m} \right\| \leq C \varepsilon_1^{-(m-2)/2}, \\ 3 \leq m \leq 4, \quad \left\| \frac{\partial^{l+m} \mathbf{X}_{r2}(x, t)}{\partial s^l \partial x^m} \right\| &\leq C, \quad 0 \leq m \leq 4. \end{aligned}$$

Case II: $\alpha \nu^2 \geq \eta \varepsilon_2$. Then, it holds

$$\begin{aligned} \left\| \frac{\partial^{l+m} \mathbf{X}_{r1}(x, t)}{\partial s^l \partial x^m} \right\| &\leq C, \quad 0 \leq m \leq 2, \quad \left\| \frac{\partial^{l+m} \mathbf{X}_{r1}(x, t)}{\partial s^l \partial x^m} \right\| \leq C \varepsilon_1^{-(m-2)}, \\ 3 \leq m \leq 4, \quad \left\| \frac{\partial^{l+m} \mathbf{X}_{r2}(x, t)}{\partial s^l \partial x^m} \right\| &\leq C, \quad 0 \leq m \leq 4. \end{aligned}$$

Case III: $\eta \varepsilon_1 < \alpha \nu^2 < \eta \varepsilon_2$. Then, we have

$$\begin{aligned} \left\| \frac{\partial^{l+m} \mathbf{X}_{r1}(x, t)}{\partial s^l \partial x^m} \right\| &\leq C, \quad 0 \leq m \leq 2, \quad \left\| \frac{\partial^{l+m} \mathbf{X}_{r1}(x, t)}{\partial s^l \partial x^m} \right\| \leq C \varepsilon_1^{-(m-2)}, \\ 3 \leq m \leq 4, \quad \left\| \frac{\partial^{l+m} \mathbf{X}_{r2}(x, t)}{\partial s^l \partial x^m} \right\| &\leq C, \quad \varepsilon_1^{-(m-2)/2}, \quad 3 \leq m \leq 4. \end{aligned}$$

After that, we show the behavior for both singular components. To do that, we consider the layer functions $\phi_{L_k}(x)$, $\phi_{R_k}(x)$, $k = 1, 2$, given by

$$\phi_{L_1}(x) = \begin{cases} e^{-\theta_1 x}, & \alpha\nu^2 \leq \eta\varepsilon_1, \\ e^{-\kappa x}, & \alpha\nu^2 \geq \eta\varepsilon_2, \\ e^{-\kappa x}, & \eta\varepsilon_1 < \alpha\nu^2 < \eta\varepsilon_2, \end{cases} \quad \phi_{R_1}(x) = \begin{cases} e^{-\theta_1(1-x)}, & \alpha\nu^2 \leq \eta\varepsilon_1, \\ e^{-\lambda_1(1-x)}, & \alpha\nu^2 \geq \eta\varepsilon_2, \\ e^{-\lambda_1(1-x)}, & \eta\varepsilon_1 < \alpha\nu^2 < \eta\varepsilon_2, \end{cases} \quad (2.3a)$$

$$\phi_{L_2}(x) = \begin{cases} e^{-\theta_2 x}, & \alpha\nu^2 \leq \eta\varepsilon_1, \\ e^{-\kappa x}, & \alpha\nu^2 \geq \eta\varepsilon_2, \\ e^{-\theta_2 x}, & \eta\varepsilon_1 < \alpha\nu^2 < \eta\varepsilon_2, \end{cases} \quad \phi_{R_2}(x) = \begin{cases} e^{-\theta_2(1-x)}, & \alpha\nu^2 \leq \eta\varepsilon_1, \\ e^{-\lambda_2(1-x)}, & \alpha\nu^2 \geq \eta\varepsilon_2, \\ e^{-\lambda_2(1-x)}, & \eta\varepsilon_1 < \alpha\nu^2 < \eta\varepsilon_2, \end{cases} \quad (2.3b)$$

where $\theta_k = \sqrt{\frac{\eta\alpha}{\varepsilon_k}}$, $\lambda_k = \frac{\alpha\nu}{\varepsilon_k}$, $\kappa = \frac{\eta}{2\nu}$, for $k = 1, 2$.

Lemma 2.5 *The layer components \mathbf{X}_L , \mathbf{X}_R satisfy the following bounds.*

Case I: $\alpha\nu^2 \leq \eta\varepsilon_1$. Then, we have

$$|\mathbf{X}_{L_1}(x, t)| \leq C\phi_{L_2}(x), |\mathbf{X}_{L_2}(x, t)| \leq C\phi_{L_2}(x), |\mathbf{X}_{R_1}(x, t)| \leq C\phi_{R_2}(x), |\mathbf{X}_{R_2}(x, t)| \leq C\phi_{R_2}(x).$$

Case II: $\alpha\nu^2 \geq \eta\varepsilon_2$. Then, it holds

$$|\mathbf{X}_{L_1}(x, t)| \leq C\phi_{L_2}(x), |\mathbf{X}_{L_2}(x, t)| \leq C\phi_{L_2}(x), |\mathbf{X}_{R_1}(x, t)| \leq C, |\mathbf{X}_{R_2}(x, t)| \leq C.$$

Case III: $\eta\varepsilon_1 < \alpha\nu^2 < \eta\varepsilon_2$. Then, we have

$$|\mathbf{X}_{L_1}(x, t)| \leq C\phi_{L_1}(x), |\mathbf{X}_{L_2}(x, t)| \leq C\phi_{L_2}(x), |\mathbf{X}_{R_1}(x, t)| \leq C\phi_{R_1}(x), |\mathbf{X}_{R_2}(x, t)| \leq C\phi_{R_2}(x).$$

Proof Using the same methodology as described in [26], the proof may be completed. \square

3 The fully discrete method

In this section, we construct the numerical method used to solve the continuous problem (1.1). To do that, first we discretize in time and later on we discretize in space the resulting problems of the time discretization.

3.1 Time-dependent discretization

Here, the Crank-Nicolson method, defined on a uniform mesh, is used to discretize the time variable. We include the necessary details to understand how the method is constructed and also we give the result proving the uniform convergence of this discretization; full details can be found in [20].

Due to the delay in time, we must use an interpolation/extrapolation to calculate the grid points, necessary to define $s - \tau$ in terms of the computational grid points and also to calculate $\mathbf{X}(x, s - \tau)$. To do that, we use the following algorithm

1. Let \mathcal{N}_s be a given positive integer. Define the mesh set $\Omega_s^{\mathcal{N}_s}$ in the s -direction as:

$$\Omega_s^{\mathcal{N}_s} = \{s_n = n \Delta s \mid n = 0, 1, \dots, \mathcal{N}_s\},$$

where $\Delta s = \frac{1}{\mathcal{N}_s}$ is the uniform step size in the s -domain.

2. Choose a delay parameter $\tau > 0$.
3. Define the function $\mathbf{X}(x, s)$ over the interval $s \in [-\tau, 0]$ and along the spatial boundaries using:

$$\mathbf{X}(x, s) = \phi(x, s), \quad \text{for } -\tau \leq s \leq 0, \quad \mathbf{X}(0, s) = \varphi_l(s), \quad \mathbf{X}(1, s) = \varphi_r(s).$$

4. Compute the non-negative integer K representing the index shift due to the delay:

$$K = \left\lfloor \frac{\tau}{\Delta s} \right\rfloor,$$

where $\lfloor \cdot \rfloor$ denotes the floor function.

5. For nodes s_m with indices $m = 1, 2, \dots, K$, it holds that $0 < s_m \leq \tau$. Thus, $s_m - \tau \in (-\tau, 0]$, and the delayed term $\mathbf{X}(x, s - \tau)$ can be evaluated using the known initial condition $\phi(x, s - \tau)$.
6. For $s_l \in \{s_n \mid n = K + 1, \dots, \mathcal{N}_s - 1\}$, i.e., for values of s satisfying $\tau < s < 1$, the delayed argument $s - \tau$ lies between the mesh points s_{l-K-1} and s_{l-K} .
7. Express $s - \tau$ as a convex linear combination of the two mesh nodes bracketing it:

$$s - \tau = \mathcal{D} s_{l-K-1} + (1 - \mathcal{D}) s_{l-K}, \quad K + 1 \leq l < \mathcal{N}_s,$$

where the weight \mathcal{D} is given by:

$$\mathcal{D} = \frac{s_{l-K} - s_l + \tau}{\Delta s} \geq 0.$$

8. Using linear interpolation, approximate the delayed function value as:

$$\mathbf{X}(x, s - \tau) \approx \mathcal{D} \mathbf{X}(x, s_{l-K-1}) + (1 - \mathcal{D}) \mathbf{X}(x, s_{l-K}), \quad K + 1 \leq l < \mathcal{N}_s.$$

Note 1. If $\tau < \Delta s$, then $K = 0$, and $s - \tau$ lies within the interval (s_{l-1}, s_l) . In such cases, $\mathbf{X}(x, s - \tau)$ is determined by interpolating between the adjacent nodes.

Note 2. If $\tau > 0$ and the value $s - \tau$ is exactly one of the mesh nodes in $\bar{\Omega}_s^{\mathcal{N}_s}$, then there exists an index l such that $s - \tau = s_{l-K}$. This yields $\mathcal{D} = 0$, meaning interpolation is unnecessary. However, this is not typically the case, and interpolation is generally required.

Then, at the $(m + 1)$ -th time level, the Crank-Nicolson method, for the components \tilde{X}_k^{n+1} , $k = 1, 2$, is defined as

$$\widetilde{\mathbf{X}}_k^{n+1}(x) = \phi(x, s_{n+1}), x \in \Omega_b, (-K+1) \leq n < 0, \quad (3.1a)$$

$$\mathbb{L}_k \widetilde{\mathbf{X}}^{n+1}(x) \equiv -\frac{\epsilon_k}{2} (\widetilde{X}_{xx}^{n+1})_k(x) - \nu \frac{p_{kk}^{n+\frac{1}{2}}(x)}{2} (\widetilde{X}_x^{n+1})_k(x) + \left(\frac{1}{\Delta s} + \frac{q_{kk}^{n+\frac{1}{2}}(x)}{2} \right) \widetilde{X}_k^{n+1}(x),$$

$$+ \frac{q_{lk}^{n+\frac{1}{2}}(x)}{2} \widetilde{X}_l^{n+1}(x) = g_k^{n+1}(x), \quad l \neq k, \quad (3.1b)$$

$$\widetilde{X}_k^{n+1}(0) = \varphi_{l_k}(s_{n+1}), \quad \widetilde{X}_k^{n+1}(1) = \varphi_{r_k}(s_{n+1}), \quad n \geq 0, \quad (3.1c)$$

where

$$g_k^{n+1}(x) = f_k^{n+\frac{1}{2}}(x) + \frac{\epsilon_k}{2} (\widetilde{X}_{xx}^n)_k(x) + \nu \frac{p_{kk}^{n+\frac{1}{2}}(x)}{2} \widetilde{X}_k^n(x) + \left(\frac{1}{\Delta s} - \frac{q_{kk}^{n+\frac{1}{2}}(x)}{2} \right) \widetilde{X}_k^n(x) - \frac{q_{lk}^{n+\frac{1}{2}}(x)}{2} \widetilde{X}_l^n(x). \quad (3.2)$$

We remember that the local truncation error is defined as $\mathcal{E}^{n+1} = \mathbf{X}(x, s_{n+1}) - \widetilde{\mathbf{X}}^{n+1}(x)$, where $\widetilde{\mathbf{X}}^{n+1}(x)$ is the solution given by (3.1) changing in (3.2) \widetilde{X}^n by the exact solution $\mathbf{X}(x, s_n)$.

On the other hand the global error is given by $\mathcal{G}^n = \mathbf{X}(x, s_n) - \widetilde{\mathbf{X}}^n$.

Theorem 3.1 *The local truncation error and the global error, associated to the Crank-Nicolson method, satisfy*

$$\|\mathcal{E}^{n+1}\| \leq C(\Delta s)^3 \quad \text{and} \quad \|\mathcal{G}^n\| \leq C(\Delta s)^{3/2}, \quad n \leq \frac{T}{\Delta s}, \quad \text{respectively}. \quad (3.3)$$

Proof Full details of the proof of this result can be seen, by instance, in [5]. □

Remark 3.2 *The order reduction from 2 to 3/2 in previous result is due to the uniform stability of the Crank-Nicolson method (see [5]). Nevertheless, as we will see in the numerical experiments section, from a numerical point of view, this reduction does not appear and the order of convergence in time is two.*

3.2 Asymptotic behavior of the solution of the semidiscrete problems

Now, we analyze which is the asymptotic behavior of the exact solution of the problems (3.1) resulting from the time semidiscretization. To do that, first we decompose

its exact solution in the form $\widetilde{\mathbf{X}}^{n+1}(x) = \widetilde{\mathbf{X}}_r^{n+1}(x) + \widetilde{\mathbf{X}}_L^{n+1}(x) + \widetilde{\mathbf{X}}_R^{n+1}(x)$, just like in (2.2).

Lemma 3.3 *Let $\widetilde{\mathbf{X}}_r^{n+1}(x) = (\widetilde{\mathbf{X}}_{r_1}^{n+1}(x), \widetilde{\mathbf{X}}_{r_2}^{n+1}(x))^T$ the regular component. Then:*

- If $\alpha \nu^2 \leq \eta \varepsilon_1$, we have

$$\left\| \frac{\partial^l \tilde{\mathbf{X}}_{r_1}^{n+1}}{\partial x^l} \right\| \leq C, \quad 0 \leq l \leq 2, \quad \left\| \frac{\partial^l \tilde{\mathbf{X}}_{r_1}^{n+1}}{\partial x^l} \right\| \leq C \varepsilon_1^{-(l-2)/2}, \quad 3 \leq l \leq 4, \quad \left\| \frac{\partial^l \tilde{\mathbf{X}}_{r_2}^{n+1}}{\partial x^l} \right\| \leq C, \quad 0 \leq l \leq 4. \quad (3.4)$$

- If $\alpha \nu^2 \geq \eta \varepsilon_2$, it holds

$$\left\| \frac{\partial^l \tilde{\mathbf{X}}_r^{n+1}}{\partial x^l} \right\| \leq C, \quad 0 \leq l \leq 2, \quad \left\| \frac{\partial^l \tilde{\mathbf{X}}_{r_1}^{n+1}}{\partial x^l} \right\| \leq C \varepsilon_1^{-(l-2)}, \quad \left\| \frac{\partial^l \tilde{\mathbf{X}}_{r_2}^{n+1}}{\partial x^l} \right\| \leq C, \quad 3 \leq l \leq 4. \quad (3.5)$$

- Finally, if $\eta \varepsilon_1 < \alpha \nu^2 < \eta \varepsilon_2$, we have

$$\left\| \frac{\partial^l \tilde{\mathbf{X}}_r^{n+1}}{\partial x^l} \right\| \leq C, \quad 0 \leq l \leq 2, \quad \left\| \frac{\partial^l \tilde{\mathbf{X}}_{r_1}^{n+1}}{\partial x^l} \right\| \leq C \varepsilon_1^{-(l-2)}, \quad \left\| \frac{\partial^l \tilde{\mathbf{X}}_{r_2}^{n+1}}{\partial x^l} \right\| \leq C \varepsilon_2^{-(l-2)/2}, \quad 3 \leq l \leq 4. \quad (3.6)$$

In second place, we show the estimates for the boundary layers function $\tilde{\mathbf{X}}_L^{n+1}(x)$ and $\tilde{\mathbf{X}}_R^{n+1}(x)$.

Lemma 3.4 Let $\tilde{\mathbf{X}}_L^{n+1}(x) = (\tilde{\mathbf{X}}_{L_1}^{n+1}(x), \tilde{\mathbf{X}}_{L_2}^{n+1}(x))^T$ and $\tilde{\mathbf{X}}_R^{n+1}(x) = (\tilde{\mathbf{X}}_{R_1}^{n+1}(x), \tilde{\mathbf{X}}_{R_2}^{n+1}(x))^T$ the left and right boundary layer functions, respectively. Then

- If $\alpha \nu^2 \leq \eta \varepsilon_1$, we have

$$\begin{aligned} |\tilde{\mathbf{X}}_{L_1}^{n+1}(x)| &\leq C \phi_{L_2}(x), \quad |\tilde{\mathbf{X}}_{L_2}^{n+1}(x)| \leq C \phi_{L_2}(x), \\ \left| \frac{\partial^l \tilde{\mathbf{X}}_{L_1}^{n+1}(x)}{\partial x^l} \right| &\leq C(\varepsilon_1^{-l/2} \phi_{L_1}(x) + \varepsilon_2^{-l/2} \phi_{L_2}(x)), \quad 1 \leq l \leq 4, \\ \left| \frac{\partial^l \tilde{\mathbf{X}}_{L_2}^{n+1}(x)}{\partial x^l} \right| &\leq C \varepsilon_2^{-l/2} \phi_{L_2}(x), \quad 1 \leq l \leq 2, \\ \left| \frac{\partial^l \tilde{\mathbf{X}}_{L_2}^{n+1}(x)}{\partial x^l} \right| &\leq C \varepsilon_2^{-1} (\varepsilon_1^{-(l-2)/2} \phi_{L_1}(x) + \varepsilon_2^{-(l-2)/2} \phi_{L_2}(x)), \quad 3 \leq l \leq 4, \\ |\tilde{\mathbf{X}}_{R_1}^{n+1}(x)| &\leq C \phi_{R_2}(x), \quad |\tilde{\mathbf{X}}_{R_2}^{n+1}(x)| \leq C \phi_{L_2}(x), \\ \left| \frac{\partial^l \tilde{\mathbf{X}}_{R_1}^{n+1}(x)}{\partial x^l} \right| &\leq C(\varepsilon_1^{-l/2} \phi_{R_1}(x) + \varepsilon_2^{-l/2} \phi_{R_2}(x)), \quad 1 \leq l \leq 4, \\ \left| \frac{\partial^l \tilde{\mathbf{X}}_{R_2}^{n+1}(x)}{\partial x^l} \right| &\leq C \varepsilon_2^{-l/2} \phi_{R_2}(x), \quad 1 \leq l \leq 2, \\ \left| \frac{\partial^l \tilde{\mathbf{X}}_{R_2}^{n+1}(x)}{\partial x^l} \right| &\leq C \varepsilon_2^{-1} (\varepsilon_1^{-(l-2)/2} \phi_{R_1}(x) + \varepsilon_2^{-(l-2)/2} \phi_{R_2}(x)), \quad 3 \leq l \leq 4. \end{aligned}$$

- If $\alpha \nu^2 \geq \eta \varepsilon_2$, it holds

$$\begin{aligned}
 |\tilde{\mathbf{X}}_{L_1}^{n+1}(x)| &\leq C\phi_{L_2}(x), |\tilde{\mathbf{X}}_{L_2}^{n+1}(x)| \leq C\phi_{L_2}(x), \\
 \left| \frac{\partial^l \tilde{\mathbf{X}}_{L_1}^{n+1}(x)}{\partial x^l} \right| &\leq C\nu^l(\varepsilon_1^{-l}\phi_{L_1}(x) + \varepsilon_2^{-l}\phi_{L_2}(x)), 1 \leq l \leq 4, \\
 \left| \frac{\partial^l \tilde{\mathbf{X}}_{L_2}^{n+1}(x)}{\partial x^l} \right| &\leq C\nu^l\varepsilon_2^{-l}\phi_{L_2}(x), 1 \leq l \leq 2, \\
 \left| \frac{\partial^3 \tilde{\mathbf{X}}_{L_2}^{n+1}(x)}{\partial x^3} \right| &\leq C\left(\frac{\nu^3}{\varepsilon_1\varepsilon_2^3}\phi_{L_1}(x) + \frac{\nu^3}{\varepsilon_2^3}\phi_{L_2}(x)\right), \\
 \left| \frac{\partial^4 \tilde{\mathbf{X}}_{L_2}^{n+1}(x)}{\partial x^4} \right| &\leq C\left(\frac{\nu^4}{\varepsilon_1\varepsilon_2^3}\phi_{L_1}(x) + \frac{\nu^4}{\varepsilon_2^4}\phi_{L_2}(x)\right), \\
 |\tilde{\mathbf{X}}_{R_1}^{n+1}(x)| &\leq C\phi_{R_2}(x), |\tilde{\mathbf{X}}_{R_2}^{n+1}(x)| \leq C\phi_{R_2}(x), \\
 \left| \frac{\partial^l \tilde{\mathbf{X}}_{R_1}^{n+1}(x)}{\partial x^l} \right| &\leq C(\varepsilon_1^{-l/2}\phi_{R_1}(x) + \varepsilon_2^{-l/2}\phi_{R_2}(x)), 1 \leq l \leq 4, \\
 \left| \frac{\partial^l \tilde{\mathbf{X}}_{R_2}^{n+1}(x)}{\partial x^l} \right| &\leq C\varepsilon_2^{-l/2}\phi_{R_2}(x), 1 \leq l \leq 2, \\
 \left| \frac{\partial^l \tilde{\mathbf{X}}_{R_2}^{n+1}(x)}{\partial x^l} \right| &\leq C\varepsilon_2^{-1}(\varepsilon_1^{-(l-2)/2}\phi_{R_1}(x) + \varepsilon_2^{-(l-2)/2}\phi_{R_2}(x)), 3 \leq l \leq 4.
 \end{aligned}$$

- Finally, if $\eta \varepsilon_1 < \alpha \nu^2 < \eta \varepsilon_2$, we have

$$\begin{aligned}
 |\tilde{\mathbf{X}}_{L_1}^{n+1}(x)| &\leq C\phi_{L_1}(x), |\tilde{\mathbf{X}}_{L_2}^{n+1}(x)| \leq C\phi_{L_2}(x), \\
 \left| \frac{\partial^l \tilde{\mathbf{X}}_{L_1}^{n+1}(x)}{\partial x^l} \right| &\leq C(\nu^l\varepsilon_1^{-l}\phi_{L_1}(x) + \varepsilon_2^{-l/2}\phi_{L_2}(x)), 1 \leq l \leq 4, \\
 \left| \frac{\partial^l \tilde{\mathbf{X}}_{L_2}^{n+1}(x)}{\partial x^l} \right| &\leq C\varepsilon_2^{-l/2}\phi_{L_2}(x), 1 \leq l \leq 2, \\
 \left| \frac{\partial^l \tilde{\mathbf{X}}_{L_2}^{n+1}(x)}{\partial x^l} \right| &\leq C\varepsilon_2^{-1}(\nu\varepsilon_1^{-(l-2)}\phi_{L_1}(x) + \varepsilon_2^{-(l-2)/2}\phi_{L_2}(x)), 3 \leq l \leq 4, \\
 |\tilde{\mathbf{X}}_{R_1}^{n+1}(x)| &\leq C\phi_{R_2}(x), |\tilde{\mathbf{X}}_{R_2}^{n+1}(x)| \leq C\phi_{R_2}(x), \\
 \left| \frac{\partial^l \tilde{\mathbf{X}}_{R_1}^{n+1}(x)}{\partial x^l} \right| &\leq C(\varepsilon_1^{-l/2}\phi_{R_1}(x) + \varepsilon_2^{-l/2}\phi_{R_2}(x)), 1 \leq l \leq 4, \\
 \left| \frac{\partial^l \tilde{\mathbf{X}}_{R_2}^{n+1}(x)}{\partial x^l} \right| &\leq C\varepsilon_2^{-l/2}\phi_{R_2}(x), 1 \leq l \leq 2, \\
 \left| \frac{\partial^l \tilde{\mathbf{X}}_{R_2}^{n+1}(x)}{\partial x^l} \right| &\leq C\varepsilon_2^{-1}(\varepsilon_1^{-(l-2)/2}\phi_{R_1}(x) + \varepsilon_2^{-(l-2)/2}\phi_{R_2}(x)), 3 \leq l \leq 4.
 \end{aligned}$$

Proof The proof of this result follows the ideas and techniques used in [26], where a scalar 1D convection-diffusion problem with parameters in the diffusion and convection terms was analyzed, and also those ones developed in [9] where a 2D elliptic system having parameters in the diffusion and convection terms was studied. \square

From the estimates given in Lemmas 3.3 and 3.4, we have adequate bounds for the derivatives in the three different cases; they will be used posteriorly for the analysis of the uniform convergence of the spatial discretization defined below.

3.3 Shishkin mesh generation

Now, we go discretize (3.1) with respect to the spatial variable. The first step to do that is the construction of an adequate nonuniform mesh, which permits concentrate the grid points in the boundary layer regions. Then, we consider the three different cases analyzed previously in Section 2. The construction of the mesh follows literally the ideas given in [9]. Let N_x an integer positive multiple of 8.

Case 1: If $\alpha \nu^2 \leq \eta \varepsilon_1$, we subdivide the unit interval into five subintervals each as

$$[0, 1] = [0, \tau_1] \cup [\tau_1, \tau_2] \cup [\tau_2, 1 - \tau_2] \cup [1 - \tau_2, 1 - \tau_1] \cup [1 - \tau_1, 1],$$

where the transition points τ_1 and τ_2 are defined by

$$\tau_1 = \min \left\{ \frac{\tau_2}{2}, \sqrt{\frac{\varepsilon_1}{\alpha \eta}} \ln N_x \right\}, \quad \tau_2 = \min \left\{ \frac{1}{4}, \sqrt{\frac{\varepsilon_2}{\alpha \eta}} \ln N_x \right\}. \quad (3.7)$$

There are $N_x/8 + 1$ uniformly spaced grid points on each of the subintervals $[0, \tau_1]$, $[\tau_1, \tau_2]$, $[1 - \tau_2, 1 - \tau_1]$, and $[1 - \tau_1, 1]$. On the remaining subinterval $[\tau_2, 1 - \tau_2]$, there are $N_x/2 + 1$ uniformly spaced grid points. Next, along the x -axis, the grid points are provided by

$$x_i = \begin{cases} \frac{8i}{N_x} \tau_1, & \text{if } 0 \leq i \leq N_x/8, \\ \tau_1 + \frac{8}{N_x} (\tau_2 - \tau_1) (i - \frac{N_x}{8}), & \text{if } N_x/8 + 1 \leq i \leq N_x/4, \\ \tau_2 + \frac{2}{N_x} (1 - 2\tau_2) (i - \frac{N_x}{4}), & \text{if } N_x/4 + 1 \leq i \leq 3N_x/4, \\ 1 - \tau_2 + \frac{8}{N_x} (\tau_2 - \tau_1) (i - \frac{3N_x}{4}), & \text{if } 3N_x/4 + 1 \leq i \leq 7N_x/8, \\ 1 - \tau_1 + \frac{8}{N_x} \tau_1 (i - \frac{7N_x}{8}), & \text{if } 7N_x/8 + 1 \leq i \leq N_x. \end{cases}$$

Case 2: If $\alpha \nu^2 \geq \eta \varepsilon_2$, then, the unit interval is divided into four subintervals each by the appropriate fitted non-uniform Shishkin mesh each as

$$[0, 1] = [0, \tau_1] \cup [\tau_1, \tau_2] \cup [\tau_2, 1 - \sigma_1] \cup [1 - \sigma_1, 1],$$

where now the transition points τ_1 , τ_2 and σ_1 are defined by

$$\tau_1 = \min \left\{ \frac{\tau_2}{2}, \frac{\varepsilon_1}{\nu\alpha} \ln N_x \right\}, \quad \tau_2 = \min \left\{ \frac{1}{4}, \frac{\varepsilon_2}{\nu\alpha} \ln N_x \right\}, \quad \sigma_1 = \min \left\{ \frac{1}{4}, \frac{\nu}{\eta} \ln N_x \right\}. \quad (3.8)$$

There are $N_x/2 + 1$ evenly spaced grid points on the subinterval $[\tau_2, 1 - \sigma_1]$, whereas the remaining subinterval $[0, \tau_1]$, $[\tau_1, \tau_2]$ there are $N_x/8 + 1$ uniformly spaced grid points, and $N_x/4 + 1$ uniformly spaced grid points on the subinterval $[1 - \sigma_1, 1]$. Next, along the x -axis, the mesh points are provided by

$$x_i = \begin{cases} \frac{8i}{N_x} \tau_1, & \text{if } 0 \leq i \leq N_x/8, \\ \tau_1 + \frac{8}{N_x} (\tau_2 - \tau_1) \left(i - \frac{N_x}{8} \right), & \text{if } N_x/8 + 1 \leq i \leq N_x/4, \\ \tau_2 + \frac{2}{N_x} (1 - \tau_2 - \sigma_1) \left(i - \frac{N_x}{4} \right), & \text{if } N_x/4 + 1 \leq i \leq 3N_x/4, \\ 1 - \sigma_1 + \frac{4}{N_x} \sigma_1 \left(i - \frac{3N_x}{4} \right), & \text{if } 3N_x/4 + 1 \leq i \leq N_x. \end{cases}$$

Case 3: If $\eta \varepsilon_1 < \alpha \nu^2 < \eta \varepsilon_2$, then, the unit interval $[0, 1]$ is divided into five subintervals each by the piecewise uniform Shishkin mesh each as

$$[0, 1] = [0, \tau_1] \cup [\tau_1, \tau_2] \cup [\tau_2, 1 - \tau_2] \cup [1 - \tau_2, 1 - \sigma_1] \cup [1 - \sigma_1, 1],$$

where σ_1 and τ_1, τ_2 are the transition points, which are now defined by

$$\tau_1 = \min \left\{ \frac{\tau_2}{2}, \frac{\varepsilon_1}{\nu\alpha} \ln N_x \right\}, \quad \tau_2 = \min \left\{ \frac{1}{4}, \sqrt{\frac{\varepsilon_2}{\alpha\eta}} \ln N_x \right\}, \quad \sigma_1 = \min \left\{ \frac{\tau_2}{2}, \frac{\nu}{\eta} \ln N_x \right\}. \quad (3.9)$$

There are $N_x/8 + 1$ uniformly spaced grid points on each of the following subintervals: $[0, \tau_1]$, $[\tau_1, \tau_2]$, $[1 - \tau_2, 1 - \sigma_1]$, $[1 - \sigma_1, 1]$; on the remaining subinterval, $[\tau_2, 1 - \tau_2]$, there are $N_x/2 + 1$ uniformly spaced grid points. Next, along the x -axis, the grid points are provided by

$$x_m = \begin{cases} \frac{8m}{N_x} \tau_1, & \text{if } 0 \leq m \leq N_x/8, \\ \tau_1 + \frac{8}{N_x} (\tau_2 - \tau_1) \left(m - \frac{N_x}{8} \right), & \text{if } N_x/8 + 1 \leq m \leq N_x/4, \\ \tau_2 + \frac{2}{N_x} (1 - 2\tau_2) \left(m - \frac{N_x}{4} \right), & \text{if } N_x/4 + 1 \leq m \leq 3N_x/4, \\ 1 - \tau_2 + \frac{8}{N_x} (\tau_2 - \sigma_1) \left(m - \frac{3N_x}{4} \right), & \text{if } 3N_x/4 + 1 \leq m \leq 7N_x/8, \\ 1 - \tau_1 + \frac{8}{N_x} \sigma_1 \left(m - \frac{7N_x}{8} \right), & \text{if } 7N_x/8 + 1 \leq m \leq N_x. \end{cases}$$

For each one of the cases, the step sizes are defined as

$$\tilde{h}_m = x_m - x_{m-1}, \quad m = 1, 2, \dots, N_x.$$

3.4 The spatial discretization

We now construct the spatial discretization on the previous Shishkin mesh, by using \mathcal{B} -splines (see [13] by instance). As it is usual, to ensure the continuity at the domain boundaries, four fictitious nodes, $x_{-2}, x_{-1}, x_{N_x+1}$ and

x_{N_x+2} , must be introduced. The nodes x_{-2} and x_{-1} are placed on the left side of Λ^{N_x} , while x_{N_x+1} and x_{N_x+2} are positioned on the right side such that $x_{-1} = x_0 - h_1$, $x_{-2} = x_{-1} - h_2$, $x_{N_x+1} = x_{N_x} + h_{N_x-1}$, $x_{N_x+2} = x_{N_x+1} + h_{N_x-2}$.

It is well known (see [16, 18] for instance) that the \mathcal{B} -splines are given by

$$\mathcal{B}_m(x) = \frac{1}{\tilde{h}_m^3} \begin{cases} (x - x_{m-2})^3, & x_{m-2} \leq x \leq x_{m-1}, \\ \tilde{h}_m^3 + 3\tilde{h}_m^2(x - x_{m-1}) + 3\tilde{h}_m(x - x_{m-1})^2 - 3(x - x_{m-1})^3, & x_{m-1} \leq x \leq x_m, \\ \tilde{h}_m^3 + 3\tilde{h}_m^2(x_{m+1} - x) + 3\tilde{h}_m(x_{m+1} - x)^2 - 3(x_{m+1} - x)^3, & x_m \leq x \leq x_{m+1}, \\ (x_{m+2} - x)^3, & x_{m+1} \leq x \leq x_{m+2}, \\ 0, & \text{otherwise.} \end{cases}$$

Then, to obtain an approximate numerical solution at time s_{n+1} we consider the function

$$\mathcal{X}_k^{n+1}(x) = \sum_{m=-1}^{N_x+1} w_{m;k}^{n+1} \mathcal{B}_m(x). \quad (3.10)$$

A system of linear equations for the unknown coefficients is obtained by substituting the \mathcal{B} -spline representation into the discretized version of the governing equations (Eq. (3.1)). Then, from [20], we have

$$\begin{aligned} \mathcal{L}_1 \mathcal{X}^{n+1} \equiv_{m=1;1}^{n+1} & \left[\frac{-\varepsilon_1}{2\tilde{h}_m^2} + \nu \frac{p_{11}^{n+\frac{1}{2}}(x_m)}{4\tilde{h}_m} + \frac{1}{6} \left(\frac{1}{\Delta s} + \frac{q_{11}^{n+\frac{1}{2}}(x_m)}{2} \right) \right] + w_{m;1}^{n+1} \left[\frac{\varepsilon_1}{\tilde{h}_m^2} + \frac{2}{3} \left(\frac{1}{\Delta s} + \frac{q_{11}^{n+\frac{1}{2}}(x_m)}{2} \right) \right] \\ & + w_{m+1;1;1}^{n+1} \left[\frac{-\varepsilon_1}{2\tilde{h}_m^2} - \nu \frac{p_{11}^{n+\frac{1}{2}}(x_m)}{4\tilde{h}_m} + \frac{1}{6} \left(\frac{1}{\Delta s} + \frac{q_{11}^{n+\frac{1}{2}}(x_m)}{2} \right) \right] + w_{m+1;1;2}^{n+1} \left(\frac{q_{12}^{n+\frac{1}{2}}(x_m)}{12} \right) \\ & + w_{m;2}^{n+1} \left(\frac{q_{12}^{n+\frac{1}{2}}(x_m)}{3} \right) + w_{m+1;2}^{n+1} \left(\frac{q_{12}^{n+\frac{1}{2}}(x_m)}{12} \right) = g_1^{n+\frac{1}{2}}(x_m) + w_{m-1;1}^{n+1} \left[\frac{\varepsilon_1}{2\tilde{h}_m^2} - \nu \frac{p_{11}^{n+\frac{1}{2}}(x_m)}{4\tilde{h}_m} \right. \\ & \left. + \frac{1}{6} \left(\frac{1}{\Delta s} - \frac{q_{11}^{n+\frac{1}{2}}(x_m)}{2} \right) \right] + w_{m;1}^n \left[-\frac{\varepsilon_1}{\tilde{h}_m^2} + \frac{2}{3} \left(\frac{1}{\Delta s} - \frac{q_{11}^{n+\frac{1}{2}}(x_m)}{2} \right) \right] \\ & + w_{m+1;1}^n \left[\frac{\varepsilon_1}{2\tilde{h}_m^2} + \nu \frac{p_{11}^{n+\frac{1}{2}}(x_m)}{4\tilde{h}_m} + \frac{1}{6} \left(\frac{1}{\Delta s} - \frac{q_{11}^{n+\frac{1}{2}}(x_m)}{2} \right) \right] \\ & - w_{m-1;2}^n \left(\frac{q_{12}^{n+\frac{1}{2}}(x_m)}{12} \right) - w_{m;2}^n \left(\frac{q_{12}^{n+\frac{1}{2}}(x_m)}{3} \right) - w_{m+1;2}^n \left(\frac{q_{12}^{n+\frac{1}{2}}(x_m)}{12} \right), \end{aligned} \quad (3.11a)$$

$$\begin{aligned} \mathcal{L}_2 \mathcal{X}^{n+1} \equiv_{m=1;1}^{n+1} & \left(\frac{q_{21}^{n+\frac{1}{2}}(x_m)}{12} \right) + w_{m;1}^{n+1} \left(\frac{q_{21}^{n+\frac{1}{2}}(x_m)}{3} \right) + w_{m+1;1}^{n+1} \left(\frac{q_{21}^{n+\frac{1}{2}}(x_m)}{12} \right) + w_{m-1;2}^{n+1} \left[\frac{-\varepsilon_2}{2\tilde{h}_m^2} + \nu \frac{p_{22}^{n+\frac{1}{2}}(x_m)}{4\tilde{h}_m} \right. \\ & \left. + \frac{1}{6} \left(\frac{1}{\Delta s} + \frac{q_{22}^{n+\frac{1}{2}}(x_m)}{2} \right) \right] + w_{m;2}^{n+1} \left[\frac{\varepsilon_2}{\tilde{h}_m^2} + \frac{2}{3} \left(\frac{1}{\Delta s} + \frac{q_{22}^{n+\frac{1}{2}}(x_m)}{2} \right) \right] + w_{m+1;2}^{n+1} \left[\frac{-\varepsilon_2}{2\tilde{h}_m^2} - \nu \frac{p_{22}^{n+\frac{1}{2}}(x_m)}{4\tilde{h}_m} \right. \\ & \left. + \frac{1}{6} \left(\frac{1}{\Delta s} + \frac{q_{22}^{n+\frac{1}{2}}(x_m)}{2} \right) \right] = g_2^{n+\frac{1}{2}}(x_m) - w_{m-1;1}^n \left(\frac{q_{21}^{n+\frac{1}{2}}(x_m)}{12} \right) \\ & - w_{m;1}^n \left(\frac{q_{21}^{n+\frac{1}{2}}(x_m)}{3} \right) - w_{m+1;1}^n \left(\frac{q_{21}^{n+\frac{1}{2}}(x_m)}{12} \right) + w_{m-1;2}^n \left[\frac{\varepsilon_2}{2\tilde{h}_m^2} - \nu \frac{p_{22}^{n+\frac{1}{2}}(x_m)}{4\tilde{h}_m} + \frac{1}{6} \left(\frac{1}{\Delta s} - \frac{q_{22}^{n+\frac{1}{2}}(x_m)}{2} \right) \right] \\ & + w_{m;2}^n \left[-\frac{\varepsilon_2}{\tilde{h}_m^2} + \frac{2}{3} \left(\frac{1}{\Delta s} - \frac{q_{22}^{n+\frac{1}{2}}(x_m)}{2} \right) \right] + w_{m+1;2}^n \left[\frac{\varepsilon_2}{2\tilde{h}_m^2} + \nu \frac{p_{22}^{n+\frac{1}{2}}(x_m)}{4\tilde{h}_m} + \frac{1}{6} \left(\frac{1}{\Delta s} - \frac{q_{22}^{n+\frac{1}{2}}(x_m)}{2} \right) \right], \end{aligned} \quad (3.11b)$$

and we must solve a linear system

$$\mathcal{A}\mathbf{w}^{n+1} = \mathcal{B}, \quad (3.12)$$

where $\mathcal{B} = \mathcal{C}\mathbf{w}^n + \mathcal{D}$ and the corresponding matrices are defined by

$$\mathcal{A} = \begin{bmatrix} \mathcal{A}_1 & \mathcal{A}_2 \\ \mathcal{A}_3 & \mathcal{A}_4 \end{bmatrix}, \quad \mathcal{C} = \begin{bmatrix} \mathcal{C}_1 & \mathcal{C}_2 \\ \mathcal{C}_3 & \mathcal{C}_4 \end{bmatrix},$$

$$\mathbf{w}^{n+1} = \left(\underbrace{w_{-1,1}^{n+1}, w_{0,1}^{n+1}, \dots, w_{N_x,1}^{n+1}, w_{N_x+1,1}^{n+1}}_{1^{\text{st}} \text{ component}}, \underbrace{w_{-1,2}^{n+1}, w_{0,2}^{n+1}, \dots, w_{N_x,2}^{n+1}, w_{N_x+1,2}^{n+1}}_{2^{\text{nd}} \text{ component}} \right)^T,$$

with

$$\begin{aligned} \mathcal{A}_1 &= [1/6, 2/3, 1/6, 0, \dots, 0; \text{tridiag}(p_1(x_m), p_2(x_m), p_3(x_m)); 0, \dots, 0, 1/6, 2/3, 1/6], \\ \mathcal{A}_2 &= [0, 0, \dots, 0; \text{tridiag}(q_1(x_m), q_2(x_m), q_1(x_m)); 0, \dots, 0, 0], \\ \mathcal{A}_3 &= [0, 0, \dots, 0; \text{tridiag}(r_1(x_m), r_2(x_m), r_1(x_m)); 0, \dots, 0, 0], \\ \mathcal{A}_4 &= [1/6, 2/3, 1/6, 0, \dots, 0; \text{tridiag}(s_1(x_m), s_2(x_m), s_3(x_m)); 0, \dots, 0, 1/6, 2/3, 1/6], \\ \mathcal{C}_1 &= [0, 0, \dots, 0; \text{tridiag}(t_1(x_m), t_2(x_m), t_3(x_m)); 0, \dots, 0, 0], \\ \mathcal{C}_2 &= [0, 0, \dots, 0; \text{tridiag}(u_1(x_m), u_2(x_m), u_1(x_m)); 0, \dots, 0, 0], \\ \mathcal{C}_3 &= [0, 0, \dots, 0; \text{tridiag}(v_1(x_m), v_2(x_m), v_1(x_m)); 0, \dots, 0, 0], \\ \mathcal{C}_4 &= [0, 0, \dots, 0; \text{tridiag}(w_1(x_m), w_2(x_m), w_3(x_m)); 0, \dots, 0, 0]. \end{aligned}$$

These matrices are tridiagonal and of order $(N_x + 3) \times (N_x + 3)$, and for $m = 0, 1, \dots, N_x$, theirs elements are given by

$$\begin{aligned} p_1(x_m) &= -\frac{\varepsilon_1}{2\tilde{h}_m^2} + \nu \frac{p_{11}^{n+\frac{1}{2}}((x_m)}{4\tilde{h}_m} + \frac{1}{6} \left(\frac{1}{\Delta s} + \frac{q_{11}^{n+\frac{1}{2}}((x_m)}{2} \right), \quad p_2(x_m) = \frac{\varepsilon_1}{\tilde{h}_m^2} + \frac{2}{3} \left(\frac{1}{\Delta s} + \frac{q_{11}^{n+\frac{1}{2}}((x_m)}{2} \right), \\ p_3(x_m) &= -\frac{\varepsilon_1}{2\tilde{h}_m^2} - \nu \frac{p_{11}^{n+\frac{1}{2}}((x_m)}{4\tilde{h}_m} + \frac{1}{6} \left(\frac{1}{\Delta s} + \frac{q_{11}^{n+\frac{1}{2}}((x_m)}{2} \right), \quad q_1(x_m) = \frac{q_{12}^{n+\frac{1}{2}}((x_m)}{12}, \\ q_2(x_m) &= \frac{q_{12}^{n+\frac{1}{2}}((x_m)}{3}, \quad r_1(x_m) = \frac{q_{21}^{n+\frac{1}{2}}((x_m)}{12}, \quad r_2(x_m) = \frac{q_{21}^{n+\frac{1}{2}}((x_m)}{3}, \\ s_1(x_m) &= -\frac{\varepsilon_2}{2\tilde{h}_m^2} + \nu \frac{p_{22}^{n+\frac{1}{2}}((x_m)}{4\tilde{h}_m} + \frac{1}{6} \left(\frac{1}{\Delta s} + \frac{q_{22}^{n+\frac{1}{2}}((x_m)}{2} \right), \quad s_2(x_m) = \frac{\varepsilon_2}{\tilde{h}_m^2} + \frac{2}{3} \left(\frac{1}{\Delta s} + \frac{q_{22}^{n+\frac{1}{2}}((x_m)}{2} \right), \\ s_3(x_m) &= -\frac{\varepsilon_2}{2\tilde{h}_m^2} - \nu \frac{p_{22}^{n+\frac{1}{2}}((x_m)}{4\tilde{h}_m} + \frac{1}{6} \left(\frac{1}{\Delta s} + \frac{q_{22}^{n+\frac{1}{2}}((x_m)}{2} \right), \\ t_1(x_m) &= \frac{\varepsilon_1}{2\tilde{h}_m^2} - \nu \frac{p_{11}^{n+\frac{1}{2}}((x_m)}{4\tilde{h}_m} + \frac{1}{6} \left(\frac{1}{\Delta s} - \frac{q_{11}^{n+\frac{1}{2}}((x_m)}{2} \right), \quad t_2(x_m) = -\frac{\varepsilon_1}{\tilde{h}_m^2} + \frac{2}{3} \left(\frac{1}{\Delta s} - \frac{q_{11}^{n+\frac{1}{2}}((x_m)}{2} \right), \\ t_3(x_m) &= \frac{\varepsilon_1}{2\tilde{h}_m^2} + \nu \frac{p_{11}^{n+\frac{1}{2}}((x_m)}{4\tilde{h}_m} + \frac{1}{6} \left(\frac{1}{\Delta s} - \frac{q_{11}^{n+\frac{1}{2}}((x_m)}{2} \right), \quad u_1(x_m) = -\frac{q_{12}^{n+\frac{1}{2}}((x_m)}{12}, \\ u_2(x_m) &= -\frac{q_{12}^{n+\frac{1}{2}}((x_m)}{3}, \quad v_1((x_m) = -\frac{q_{21}^{n+\frac{1}{2}}((x_m)}{12}, \quad v_2(x_m) = -\frac{q_{21}^{n+\frac{1}{2}}((x_m)}{3}, \\ w_1(x_m) &= \frac{\varepsilon_2}{2\tilde{h}_m^2} - \nu \frac{p_{22}^{n+\frac{1}{2}}((x_m)}{4\tilde{h}_m} + \frac{1}{6} \left(\frac{1}{\Delta s} - \frac{q_{22}^{n+\frac{1}{2}}((x_m)}{2} \right), \quad w_2(x_m) = -\frac{\varepsilon_2}{\tilde{h}_m^2} + \frac{2}{3} \left(\frac{1}{\Delta s} - \frac{q_{22}^{n+\frac{1}{2}}((x_m)}{2} \right), \\ w_3(x_m) &= \frac{\varepsilon_2}{2\tilde{h}_m^2} + \nu \frac{p_{22}^{n+\frac{1}{2}}((x_m)}{4\tilde{h}_m} + \frac{1}{6} \left(\frac{1}{\Delta s} - \frac{q_{22}^{n+\frac{1}{2}}((x_m)}{2} \right), \\ \mathcal{D} &= \left(\varphi_{l_1}(s_{n+1}), g_1^{n+\frac{1}{2}}(x_0), \dots, g_1^{n+\frac{1}{2}}(x_{N_x}), \varphi_{r_1}(s_{n+1}), \varphi_{l_2}(s_{n+1}), g_2^{n+\frac{1}{2}}(x_0), \dots, g_2^{n+\frac{1}{2}}(x_{N_x}), \varphi_{r_2}(s_{n+1}) \right)^T. \end{aligned}$$

4 Uniform convergence of the numerical method

In this section we prove the uniform convergence of the numerical solution given by (3.10). In the proof we use the well known following result.

Lemma 4.1 *The cubic B-spline functions satisfy*

$$\sum_{n=-1}^{\mathcal{N}_x+1} |\mathcal{B}_n(x)| \leq 10, \quad x \in [0, 1].$$

Proof The proof may be completed using the methods outlined in [27]. \square

The first result that we will use in the proof of the uniform convergence is the discrete analogous to the maximum principle for the continuous differential operator. We denote $\mathcal{L}^{\mathcal{N}_x} = (\mathcal{L}_1, \mathcal{L}_2)^T$.

Lemma 4.2 *Let $\tilde{\Psi}^{n+1}(x_0) \geq 0, \tilde{\Psi}^{n+1}(x_{\mathcal{N}_x}) \geq 0$ and $\mathcal{L}^{\mathcal{N}_x} \tilde{\Psi}^{n+1}(x_{\mathcal{N}_x}) \leq 0$ for all $x_m \in \Lambda^{\mathcal{N}_x}$. Then, $\tilde{\Psi}^{n+1}(x_m) \geq 0$ for all $x_m \in \bar{\Lambda}^{\mathcal{N}_x}$.*

Next result gives the uniform convergence of almost second order of the spatial discretization constructed on the special piecewise uniform Shishkin mesh defined in previous section.

Theorem 4.3 *If $g \in C^2[0, 1]$ represent a generic function with continuous second derivatives, used here to indicate the required regularity for the convergence estimate, then the approximated solution $\mathbf{X}^{n+1}(x)$ to the solution $\tilde{\mathbf{X}}(x)$ of (3.1) on $\Omega_s^{\mathcal{N}_s}$ at the $(n+1)$ -th time level satisfies*

$$\sup_{0 < \varepsilon_1, \varepsilon_2, \nu \leq 1} \|\mathbf{X}^{n+1} - \tilde{\mathbf{X}}^{n+1}\| \leq C \mathcal{N}_x^{-2} (\ln \mathcal{N}_x)^2.$$

Then, the spatial discretization is an almost second order uniformly convergent method.

Proof A specific spline interpolant $\mathbf{X}_{\mathcal{N}_x}(x)$ is provided in order to solve the problem (3.1), which is given by

$$\mathbf{X}_{\mathcal{N}_x}(x) = \sum_{m=-1}^{\mathcal{N}_x+1} w_{m;l}^{n+1} \mathcal{B}_m(x).$$

Below, we represent $\tilde{\mathbf{X}}$ as $\tilde{\mathbf{X}}^{n+1}$ for simplicity's sake. From [13], we know that it holds

$$\|D^j(\tilde{\mathbf{X}} - \mathbf{X}_{\mathcal{N}_x})(x_m)\|_\infty \leq C_j \|\tilde{\mathbf{X}}^{(4)}\| \bar{h}^{4-j}, \quad j = 0, 1, 2.$$

The constants C_j and $\bar{h} = \max_m \tilde{h}_m$ are used and D^j represents the derivative of order j .

By using the decomposition

$$\tilde{\mathbf{X}}(x) = \tilde{\mathbf{X}}_r(x) + \tilde{\mathbf{X}}_L(x) + \tilde{\mathbf{X}}_R(x),$$

for the numerical solution, it immediately follows

$$\|D^j(\tilde{\mathbf{X}} - \mathbf{X}_{\mathcal{N}_x})(x_m)\|_\infty \leq C_j \|\tilde{\mathbf{X}}_r(x) + \tilde{\mathbf{X}}_L(x) + \tilde{\mathbf{X}}_R(x)^{(4)}\| \bar{h}^{4-j}, \quad j = 0, 1, 2. \quad (4.1)$$

Now, we study each one of the three different cases associated to the value and the ratio between the diffusion and the convection parameters. Firstly, we consider the regular component.

- If $\alpha \nu^2 \leq \eta \varepsilon_1$ holds, we have the estimations (4.1) and using Lemma 3.3, clearly we can obtain

$$\begin{aligned} |\mathcal{L}_1 \widetilde{\mathbf{X}}_{r_1}(x) - \mathcal{L}_1(\mathbf{X}_{r_1})_{\mathcal{N}_x}| &\leq \left(\frac{\varepsilon_1}{2} \psi_2 \bar{h}^2 + \frac{\nu}{2} \left\| p_{11}^{n+1/2} \right\| \psi_1 \bar{h}^3 + \frac{1}{2} \left\| \mathfrak{R}_1^{n+1/2} \right\| \psi_0 \bar{h}^4 \right) |\widetilde{\mathbf{X}}_{r_1}^{(4)}(x)| \\ &\leq C \left(\varepsilon_1 \psi_2 \bar{h}^2 + \nu \left\| p_{11}^{n+1/2} \right\| \psi_1 \bar{h}^3 + \left\| \mathfrak{R}_1^{n+1/2} \right\| \psi_0 \bar{h}^4 \right) \left(\frac{1}{\varepsilon_1} \right), \\ |\mathcal{L}_2 \widetilde{\mathbf{X}}_{r_2}(x) - \mathcal{L}_2(\mathbf{X}_{r_2})_{\mathcal{N}_x}| &\leq \left(\frac{\varepsilon_2}{2} \psi_2 \bar{h}^2 + \frac{\nu}{2} \left\| p_{22}^{n+1/2} \right\| \psi_1 \bar{h}^3 + \frac{1}{2} \left\| \mathfrak{R}_2^{n+1/2} \right\| \psi_0 \bar{h}^4 \right) |\widetilde{\mathbf{X}}_{r_2}^{(4)}(x)| \\ &\leq C \left(\varepsilon_2 \psi_2 \bar{h}^2 + \nu \left\| p_{22}^{n+1/2} \right\| \psi_1 \bar{h}^3 + \left\| \mathfrak{R}_2^{n+1/2} \right\| \psi_0 \bar{h}^4 \right), \end{aligned}$$

where

$$\mathfrak{R}_k^{m+\frac{1}{2}}(x) = \frac{1}{\Delta s} + \frac{q_{kk}^{m+\frac{1}{2}}(x)}{2}.$$

Using that $\bar{h} = \frac{1}{\mathcal{N}_x}$, we get

$$|\mathcal{L}_1 \widetilde{\mathbf{X}}_r(x) - \mathcal{L}_1(\mathbf{X}_r)_{\mathcal{N}_x}| \leq C \mathcal{N}_x^{-2}, \quad (4.2)$$

and also

$$|\mathcal{L}_2 \widetilde{\mathbf{X}}_r(x) - \mathcal{L}_2(\mathbf{X}_r)_{\mathcal{N}_x}| \leq C \mathcal{N}_x^{-2}. \quad (4.3)$$

Then, we finally have

$$|\mathcal{L}^{\mathcal{N}_x} \mathcal{X}_r^{n+1} - \mathcal{L}^{\mathcal{N}_x}(\mathbf{X})_{r\mathcal{N}_x}| \leq C\mathcal{N}_x^{-2}. \quad (4.4)$$

- If $\alpha \nu^2 \geq \eta \varepsilon_2$, we have

$$\begin{aligned} |\mathcal{L}_1 \widetilde{\mathbf{X}}_{r_1}(x) - \mathcal{L}_1(\mathbf{X}_{r_1})_{\mathcal{N}_x}| &\leq \left(\frac{\varepsilon_1}{2} \psi_2 \bar{h}^2 + \frac{\nu}{2} \left\| p_{11}^{n+1/2} \right\| \psi_1 \bar{h}^3 + \frac{1}{2} \left\| \mathfrak{R}_1^{n+1/2} \right\| \psi_0 \bar{h}^4 \right) |\widetilde{\mathbf{X}}_{r_1}^{(4)}(x)| \\ &\leq C \left(\varepsilon_1 \psi_2 \bar{h}^2 + \nu \left\| p_{11}^{n+1/2} \right\| \psi_1 \bar{h}^3 + \left\| \mathfrak{R}_1^{n+1/2} \right\| \psi_0 \bar{h}^4 \right) \left(\frac{1}{\varepsilon_1} \right), \\ |\mathcal{L}_2 \widetilde{\mathbf{X}}_r(x) - \mathcal{L}_2(\mathbf{X}_r)_{\mathcal{N}_x}| &\leq \left(\frac{\varepsilon_2}{2} \psi_2 \bar{h}^2 + \frac{\nu}{2} \left\| p_{22}^{n+1/2} \right\| \psi_1 \bar{h}^3 + \frac{1}{2} \left\| \mathfrak{R}_2^{n+1/2} \right\| \psi_0 \bar{h}^4 \right) |\widetilde{\mathbf{X}}_r^{(4)}(x)| \\ &\leq C \left(\varepsilon_2 \psi_2 \bar{h}^2 + \nu \left\| p_{22}^{n+1/2} \right\| \psi_1 \bar{h}^3 + \left\| \mathfrak{R}_2^{n+1/2} \right\| \psi_0 \bar{h}^4 \right), \end{aligned}$$

Using that $\bar{h} = \frac{1}{\mathcal{N}_x}$, we get

$$|\mathcal{L}_1 \widetilde{\mathbf{X}}_r(x) - \mathcal{L}_1(\mathbf{X}_r)_{\mathcal{N}_x}| \leq C\mathcal{N}_x^{-2}. \quad (4.5)$$

and also

$$|\mathcal{L}_2 \widetilde{\mathbf{X}}_r(x) - \mathcal{L}_2(\mathbf{X}_r)_{\mathcal{N}_x}| \leq C\mathcal{N}_x^{-2}. \quad (4.6)$$

Then, we finally have

$$|\mathcal{L}^{\mathcal{N}_x} \mathcal{X}_r^{n+1} - \mathcal{L}^{\mathcal{N}_x}(\mathbf{X})_{r\mathcal{N}_x}| \leq C\mathcal{N}_x^{-2}. \quad (4.7)$$

- Finally, if $\delta \varepsilon_1 < \alpha \nu^2 < \delta \varepsilon_2$ holds, we have

$$\begin{aligned} |\mathcal{L}_1 \widetilde{\mathbf{X}}_r(x) - \mathcal{L}_1(\mathbf{X}_r)_{\mathcal{N}_x}| &\leq \left(\frac{\varepsilon_1}{2} \psi_2 \bar{h}^2 + \frac{\nu}{2} \left\| p_{11}^{n+1/2} \right\| \psi_1 \bar{h}^3 + \frac{1}{2} \left\| \mathfrak{R}_1^{n+1/2} \right\| \psi_0 \bar{h}^4 \right) |\widetilde{\mathbf{X}}_r^{(4)}(x)| \\ &\leq C \left(\varepsilon_1 \psi_2 \bar{h}^2 + \nu \left\| p_{11}^{n+1/2} \right\| \psi_1 \bar{h}^3 + \left\| \mathfrak{R}_1^{n+1/2} \right\| \psi_0 \bar{h}^4 \right) \left(\frac{1}{\varepsilon_1} \right), \\ |\mathcal{L}_2 \widetilde{\mathbf{X}}_r(x) - \mathcal{L}_2(\mathbf{X}_r)_{\mathcal{N}_x}| &\leq \left(\frac{\varepsilon_2}{2} \psi_2 \bar{h}^2 + \frac{\nu}{2} \left\| p_{22}^{n+1/2} \right\| \psi_1 \bar{h}^3 + \frac{1}{2} \left\| \mathfrak{R}_2^{n+1/2} \right\| \psi_0 \bar{h}^4 \right) |\widetilde{\mathbf{X}}_r^{(4)}(x)| \\ &\leq C \left(\varepsilon_2 \psi_2 \bar{h}^2 + \nu \left\| p_{22}^{n+1/2} \right\| \psi_1 \bar{h}^3 + \left\| \mathfrak{R}_2^{n+1/2} \right\| \psi_0 \bar{h}^4 \right) \left(\frac{1}{\varepsilon_2} \right), \end{aligned}$$

Using that $\bar{h} = \frac{1}{\mathcal{N}_x}$, we get

$$|\mathcal{L}_1 \widetilde{\mathbf{X}}_r(x) - \mathcal{L}_1(\mathbf{X}_r)_{\mathcal{N}_x}| \leq C\mathcal{N}_x^{-2}, \quad (4.8)$$

and also

$$|\mathcal{L}_2 \widetilde{\mathbf{X}}_r(x) - \mathcal{L}_2(\mathbf{X}_r)_{\mathcal{N}_x}| \leq C\mathcal{N}_x^{-2}. \quad (4.9)$$

So, we have

$$|\mathcal{L}^{\mathcal{N}_x} \mathcal{X}_r^{n+1} - \mathcal{L}^{\mathcal{N}_x}(\mathbf{X})_{r, \mathcal{N}_x}| \leq C \mathcal{N}_x^{-2}. \quad (4.10)$$

Hence, by combining (4.4), (4.7) and (4.10), we obtain

$$|\mathcal{L}^{\mathcal{N}_x} \mathcal{X}_r^{n+1} - \mathcal{L}^{\mathcal{N}_x}(\mathbf{X})_{r, \mathcal{N}_x}| \leq C \mathcal{N}_x^{-2}. \quad (4.11)$$

From (4.11) follows the uniform consistency for the regular component; then, the discrete maximum principle proves that it holds

$$|\mathcal{X}_r^{n+1} - \mathbf{X}_{r, \mathcal{N}_x}| \leq C \mathcal{N}_x^{-2}, \quad (4.12)$$

which is the required result for the regular component.

Now, we will do the analysis for $\widetilde{\mathbf{X}}_L^{n+1}(x)$; again we distinguish three cases.

• If $\alpha \nu^2 \leq \eta \varepsilon_1$ holds. The estimates (4.1) and the use of Lemma 3.4, clearly shows that

$$\begin{aligned} & |\mathcal{L}_1 \widetilde{\mathbf{X}}_{L_1}(x) - \mathcal{L}_1(\mathbf{X}_{L_1})_{\mathcal{N}_x}| \\ & \leq \left(\frac{\varepsilon_1}{2} \psi_2 \bar{h}^2 + \frac{\nu}{2} \left\| p_{11}^{n+1/2} \right\| \psi_1 \bar{h}^3 + \frac{1}{2} \left\| \mathfrak{R}_1^{n+1/2} \right\| \psi_0 \bar{h}^4 \right) |\widetilde{\mathbf{X}}_{L_1}^{(4)}(x)| \\ & \leq C \left(\varepsilon_1 \psi_2 \bar{h}^2 + \nu \left\| p_{11}^{n+1/2} \right\| \psi_1 \bar{h}^3 + \left\| \mathfrak{R}_1^{n+1/2} \right\| \psi_0 \bar{h}^4 \right) \\ & \quad (\varepsilon_1^{-2} \phi_{L_1}(x) + \varepsilon_2^{-2} \phi_{L_2}(x)), \end{aligned} \quad (4.13)$$

$$\begin{aligned} & |\mathcal{L}_2 \widetilde{\mathbf{X}}_{L_1}(x) - \mathcal{L}_2(\mathbf{X}_{L_1})_{\mathcal{N}_x}| \\ & \leq \left(\frac{\varepsilon_2}{2} \psi_2 \bar{h}^2 + \frac{\nu}{2} \left\| p_{22}^{n+1/2} \right\| \psi_1 \bar{h}^3 + \frac{1}{2} \left\| \mathfrak{R}_2^{n+1/2} \right\| \psi_0 \bar{h}^4 \right) |\widetilde{\mathbf{X}}_{L_1}^{(4)}(x)| \\ & \leq C \left(\varepsilon_2 \psi_2 \bar{h}^2 + \nu \left\| p_{22}^{n+1/2} \right\| \psi_1 \bar{h}^3 + \left\| \mathfrak{R}_2^{n+1/2} \right\| \psi_0 \bar{h}^4 \right) \\ & \quad (\varepsilon_1^{-2} \phi_{L_1}(x) + \varepsilon_2^{-2} \phi_{L_2}(x)), \end{aligned} \quad (4.14)$$

Then, if $x_m \in (0, \tau_1]$ or $[1 - \tau_1, 1)$, it holds $\exp(-\theta_1 x_m) \leq 1$ and $\exp(-\theta_2(1 - x_m)) \leq \exp(-\theta_1(1 - \tau_1)) \leq \mathcal{N}_x$. Thus, (4.13) and (4.14) yield

$$\begin{aligned} & |\mathcal{L}_1 \widetilde{\mathbf{X}}_{L_1}(x) - \mathcal{L}_1(\mathbf{X}_{L_1})_{\mathcal{N}_x}| \leq C \\ & \quad \left(\varepsilon_1 \psi_2 \bar{h}^2 + \nu \left\| p_{11}^{n+1/2} \right\| \psi_1 \bar{h}^3 + \left\| \mathfrak{R}_1^{n+1/2} \right\| \psi_0 \bar{h}^4 \right) (\varepsilon_1^{-2} + \varepsilon_2^{-2}). \end{aligned} \quad (4.15)$$

Using the suitable barrier functions, then we have

$$|\mathcal{L}_1 \widetilde{\mathbf{X}}_{L_1}(x) - \mathcal{L}_1(\mathbf{X}_{L_1})_{\mathcal{N}_x}| \leq C \mathcal{N}_x^{-2} (\ln \mathcal{N}_x)^2, \quad (4.16)$$

$$\begin{aligned} & |\mathcal{L}_2 \widetilde{\mathbf{X}}_{L_1}(x) - \mathcal{L}_2(\mathbf{X}_{L_1})_{\mathcal{N}_x}| \\ & \leq C \left(\varepsilon_2 \psi_2 \bar{h}^2 + \nu \left\| p_{22}^{n+1/2} \right\| \psi_1 \bar{h}^3 + \left\| \mathfrak{R}_2^{n+1/2} \right\| \psi_0 \bar{h}^4 \right) (\varepsilon_1^{-2} + \varepsilon_2^{-2}). \end{aligned} \quad (4.17)$$

Using the suitable barrier functions, then we have

$$|\mathcal{L}_2 \widetilde{\mathbf{X}}_{L_1}(x) - \mathcal{L}_2(\mathbf{X}_{L_1})_{\mathcal{N}_x}| \leq C \mathcal{N}_x^{-2} (\ln \mathcal{N}_x)^2. \quad (4.18)$$

If $x_m \in (\tau_1, \tau_2]$ or $(1 - \tau_2, 1 - \tau_1)$, $\bar{h} \leq C \mathcal{N}_x^{-2} \tau_2 \leq C \mathcal{N}_x^{-2} \ln \mathcal{N}_x \sqrt{\varepsilon_2}$, then we have

$$|\mathcal{L}_1 \widetilde{\mathbf{X}}_{L_1}(x) - \mathcal{L}_1(\mathbf{X}_{L_1})_{\mathcal{N}_x}| \leq C \mathcal{N}_x^{-2} \ln \mathcal{N}_x \sqrt{\varepsilon_2} (\varepsilon_1^{-2} \phi_{L_1}(x) + \varepsilon_2^{-2} \phi_{L_2}(x)),$$

and

$$|\mathcal{L}_2 \widetilde{\mathbf{X}}_{L_1}(x) - \mathcal{L}_2(\mathbf{X}_{L_1})_{\mathcal{N}_x}| \leq C \mathcal{N}_x^{-2} (\ln \mathcal{N}_x)^2 \sqrt{\varepsilon_2} (\varepsilon_1^{-2} \phi_{L_1}(x) + \varepsilon_2^{-2} \phi_{L_2}(x)).$$

Using the suitable barrier functions, then we have

$$|\mathcal{L}_1 \widetilde{\mathbf{X}}_{L_1}(x) - \mathcal{L}_1(\mathbf{X}_{L_1})_{\mathcal{N}_x}| \leq C \mathcal{N}_x^{-2} (\ln \mathcal{N}_x)^2,$$

and also

$$|\mathcal{L}_2 \widetilde{\mathbf{X}}_{L_1}(x) - \mathcal{L}_2(\mathbf{X}_{L_1})_{\mathcal{N}_x}| \leq C \mathcal{N}_x^{-2} (\ln \mathcal{N}_x)^2.$$

So, we obtain

$$|\mathcal{X}_r^{n+1} - \mathcal{L}^{\mathcal{N}_x}(\mathbf{X})_{r \mathcal{N}_x}| \leq C \mathcal{N}_x^{-2} \ln(\mathcal{N}_x)^2. \quad (4.19)$$

When $x_m \in [\tau_2, 1 - \tau_2]$, we can obtain the required bounds by using a method similar to that used in the corresponding intervals of the previous cases. So, for all $0 \leq x_m \leq \mathcal{N}_x$, we have

$$|\mathcal{X}_L^{\mathcal{N}_x} \mathcal{X}_L^{n+1} - \mathcal{L}^{\mathcal{N}_x}(\mathbf{X})_{L \mathcal{N}_x}| \leq C \mathcal{N}_x^{-2} (\ln \mathcal{N}_x)^2, \quad (4.20)$$

which is the required result for the left layer component $\widetilde{\mathbf{X}}_L^{n+1}(x)$.

By following the similar approach, we can prove the parameter uniform error estimates for the component $\widetilde{\mathbf{X}}_R^{n+1}(x)$ for this case, obtaining

$$|\mathcal{X}_R^{\mathcal{N}_x} \mathcal{X}_R^{n+1} - \mathcal{L}^{\mathcal{N}_x}(\mathbf{X})_{R \mathcal{N}_x}| \leq C \mathcal{N}_x^{-2} (\ln \mathcal{N}_x)^2. \quad (4.21)$$

- If $\alpha \nu^2 \leq \eta \varepsilon_1$ holds. The estimates (4.1) and the use of Lemma 3.4, clearly shows that

$$\begin{aligned}
& |\mathcal{L}_1 \widetilde{\mathbf{X}}_{L_1}(x) - \mathcal{L}_1(\mathbf{X}_{L_1})_{\mathcal{N}_x}| \\
& \leq \left(\frac{\varepsilon_1}{2} \psi_2 \bar{h}^2 + \frac{\nu}{2} \left\| p_{11}^{n+1/2} \right\| \psi_1 \bar{h}^3 + \frac{1}{2} \left\| \mathfrak{R}_1^{n+1/2} \right\| \psi_0 \bar{h}^4 \right) |\widetilde{\mathbf{X}}_{L_1}^{(4)}(x)| \\
& \leq C \left(\varepsilon_1 \psi_2 \bar{h}^2 + \nu \left\| p_{11}^{n+1/2} \right\| \psi_1 \bar{h}^3 + \left\| \mathfrak{R}_1^{n+1/2} \right\| \psi_0 \bar{h}^4 \right) \\
& \quad (v^4 \varepsilon_1^{-4} \phi_{L_1}(x) + v^4 \varepsilon_2^{-4} \phi_{L_2}(x)),
\end{aligned} \tag{4.22}$$

$$\begin{aligned}
& |\mathcal{L}_2 \widetilde{\mathbf{X}}_{L_1}(x) - \mathcal{L}_2(\mathbf{X}_{L_1})_{\mathcal{N}_x}| \\
& \leq \left(\frac{\varepsilon_2}{2} \psi_2 \bar{h}^2 + \frac{\nu}{2} \left\| p_{22}^{n+1/2} \right\| \psi_1 \bar{h}^3 + \frac{1}{2} \left\| \mathfrak{R}_2^{n+1/2} \right\| \psi_0 \bar{h}^4 \right) |\widetilde{\mathbf{X}}_{L_1}^{(4)}(x)| \\
& \leq C \left(\varepsilon_2 \psi_2 \bar{h}^2 + \nu \left\| p_{22}^{n+1/2} \right\| \psi_1 \bar{h}^3 + \left\| \mathfrak{R}_2^{n+1/2} \right\| \psi_0 \bar{h}^4 \right) \\
& \quad \left(\frac{v^4}{\varepsilon_1 \varepsilon_2^3} \phi_{L_1}(x) + \frac{v^4}{\varepsilon_2^4} \phi_{L_2}(x) \right),
\end{aligned} \tag{4.23}$$

Then, if $x_m \in (0, \tau_1]$ or $[1 - \tau_1, 1]$, it holds $\exp(-\theta_1 x_m) \leq 1$ and $\exp(-\theta_2(1 - x_m)) \leq \exp(-\theta_1(1 - \tau_1)) \leq \mathcal{N}_x$. Thus, (4.31) and (4.32) yield

$$\begin{aligned}
& |\mathcal{L}_1 \widetilde{\mathbf{X}}_{L_1}(x) - \mathcal{L}_1(\mathbf{X}_{L_1})_{\mathcal{N}_x}| \leq C \\
& \quad \left(\varepsilon_1 \psi_2 \bar{h}^2 + \nu \left\| p_{11}^{n+1/2} \right\| \psi_1 \bar{h}^3 + \left\| \mathfrak{R}_1^{n+1/2} \right\| \psi_0 \bar{h}^4 \right) (v^4 \varepsilon_1^{-4} + v^4 \varepsilon_2^{-4}).
\end{aligned} \tag{4.24}$$

Using the suitable barrier functions, then we have

$$|\mathcal{L}_1 \widetilde{\mathbf{X}}_{L_1}(x) - \mathcal{L}_1(\mathbf{X}_{L_1})_{\mathcal{N}_x}| \leq C \mathcal{N}_x^{-2} (\ln \mathcal{N}_x)^2, \tag{4.25}$$

$$\begin{aligned}
& |\mathcal{L}_2 \widetilde{\mathbf{X}}_{L_1}(x) - \mathcal{L}_2(\mathbf{X}_{L_1})_{\mathcal{N}_x}| \\
& \leq C \left(\varepsilon_2 \psi_2 \bar{h}^2 + \nu \left\| p_{22}^{n+1/2} \right\| \psi_1 \bar{h}^3 + \left\| \mathfrak{R}_2^{n+1/2} \right\| \psi_0 \bar{h}^4 \right) \left(\frac{v^4}{\varepsilon_1 \varepsilon_2^3} \phi_{L_1}(x) + \frac{v^4}{\varepsilon_2^4} \phi_{L_2}(x) \right)
\end{aligned} \tag{4.26}$$

Using the suitable barrier functions, then we have

$$|\mathcal{L}_2 \widetilde{\mathbf{X}}_{L_1}(x) - \mathcal{L}_2(\mathbf{X}_{L_1})_{\mathcal{N}_x}| \leq C \mathcal{N}_x^{-2} (\ln \mathcal{N}_x)^2. \tag{4.27}$$

If $x_m \in (\tau_1, \tau_2]$ or $(1 - \tau_2, 1 - \tau_1)$, $\bar{h} \leq C \mathcal{N}_x^{-2} \tau_2 \leq C \mathcal{N}_x^{-2} \ln \mathcal{N}_x \sqrt{\varepsilon_2}$, then we have

$$|\mathcal{L}_1 \widetilde{\mathbf{X}}_{L_1}(x) - \mathcal{L}_1(\mathbf{X}_{L_1})_{\mathcal{N}_x}| \leq C \mathcal{N}_x^{-2} \ln \mathcal{N}_x \sqrt{\varepsilon_2} (\varepsilon_1^{-2} \phi_{L_1}(x) + \varepsilon_2^{-2} \phi_{L_2}(x)),$$

and

$$|\mathcal{L}_2 \widetilde{\mathbf{X}}_{L_1}(x) - \mathcal{L}_2(\mathbf{X}_{L_1})_{\mathcal{N}_x}| \leq C \mathcal{N}_x^{-2} (\ln \mathcal{N}_x)^2 \sqrt{\varepsilon_2} (\varepsilon_1^{-2} \phi_{L_1}(x) + \varepsilon_2^{-2} \phi_{L_2}(x)).$$

Using the suitable barrier functions, then we have

$$|\mathcal{L}_1 \widetilde{\mathbf{X}}_{L_1}(x) - \mathcal{L}_1(\mathbf{X}_{L_1})_{\mathcal{N}_x}| \leq C \mathcal{N}_x^{-2} (\ln \mathcal{N}_x)^2,$$

and also

$$|\mathcal{L}_2 \widetilde{\mathbf{X}}_{L_1}(x) - \mathcal{L}_2(\mathbf{X}_{L_1})_{\mathcal{N}_x}| \leq C \mathcal{N}_x^{-2} (\ln \mathcal{N}_x)^2.$$

So, we can obtain

$$|\mathcal{L}^{\mathcal{N}_x} \mathcal{X}_{\mathbf{r}}^{n+1} - \mathcal{L}^{\mathcal{N}_x}(\mathbf{X})_{r \mathcal{N}_x}| \leq C \mathcal{N}_x^{-2} \ln(\mathcal{N}_x)^2. \quad (4.28)$$

When $x_m \in [\tau_2, 1 - \tau_2]$, we can obtain the required bounds by using a method similar to that used in the corresponding intervals of the previous cases. So, for all $0 \leq x_m \leq \mathcal{N}_x$, we have

$$|\mathcal{L}^{\mathcal{N}_x} \mathcal{X}_{\mathbf{L}}^{n+1} - \mathcal{L}^{\mathcal{N}_x}(\mathbf{X})_{L \mathcal{N}_x}| \leq C \mathcal{N}_x^{-2} (\ln \mathcal{N}_x)^2, \quad (4.29)$$

which is the required result for the left layer component $\widetilde{\mathbf{X}}_L^{n+1}(x)$.

By following the similar approach, we can prove the parameter uniform error estimates for the component $\widetilde{\mathbf{X}}_R^{n+1}(x)$, obtaining

$$|\mathcal{L}^{\mathcal{N}_x} \mathcal{X}_{\mathbf{R}}^{n+1} - \mathcal{L}^{\mathcal{N}_x}(\mathbf{X})_{R \mathcal{N}_x}| \leq C \mathcal{N}_x^{-2} (\ln \mathcal{N}_x)^2. \quad (4.30)$$

- Finally, if $\delta \varepsilon_1 < \alpha \nu^2 < \delta \varepsilon_2$ holds, we have

$$\begin{aligned} & |\mathcal{L}_1 \widetilde{\mathbf{X}}_{L_1}(x) - \mathcal{L}_1(\mathbf{X}_{L_1})_{\mathcal{N}_x}| \\ & \leq \left(\frac{\varepsilon_1}{2} \psi_2 \bar{h}^2 + \frac{\nu}{2} \left\| p_{11}^{n+1/2} \right\| \psi_1 \bar{h}^3 + \frac{1}{2} \left\| \mathfrak{R}_1^{n+1/2} \right\| \psi_0 \bar{h}^4 \right) |\widetilde{\mathbf{X}}_{L_1}^{(4)}(x)| \\ & \leq C \left(\varepsilon_1 \psi_2 \bar{h}^2 + \nu \left\| p_{11}^{n+1/2} \right\| \psi_1 \bar{h}^3 + \left\| \mathfrak{R}_1^{n+1/2} \right\| \psi_0 \bar{h}^4 \right) \\ & \quad (\nu^4 \varepsilon_1^{-4} \phi_{L_1}(x) + \varepsilon_2^{-2} \phi_{L_2}(x)), \end{aligned} \quad (4.31)$$

$$\begin{aligned}
& |\mathcal{L}_2 \widetilde{\mathbf{X}}_{L_1}(x) - \mathcal{L}_2(\mathbf{X}_{L_1})_{\mathcal{N}_x}| \\
& \leq \left(\frac{\varepsilon_2}{2} \psi_2 \bar{h}^2 + \frac{\nu}{2} \left\| p_{22}^{n+1/2} \right\| \psi_1 \bar{h}^3 + \frac{1}{2} \left\| \mathfrak{R}_2^{n+1/2} \right\| \psi_0 \bar{h}^4 \right) |\widetilde{\mathbf{X}}_{L_1}^{(4)}(x)| \\
& \leq C \left(\varepsilon_2 \psi_2 \bar{h}^2 + \nu \left\| p_{22}^{n+1/2} \right\| \psi_1 \bar{h}^3 + \left\| \mathfrak{R}_2^{n+1/2} \right\| \psi_0 \bar{h}^4 \right) \\
& \quad (\varepsilon_2^{-1} \varepsilon_1^{-2} \nu \phi_{L_1}(x) + \varepsilon_2^{-3} \phi_{L_2}(x)).
\end{aligned} \tag{4.32}$$

Then, if $x_m \in (0, \tau_1]$ or $[1 - \tau_1, 1]$, it holds $\exp(-\theta_1 x_m) \leq 1$ and $\exp(-\theta_2(1 - x_m)) \leq \exp(-\theta_1(1 - \tau_1)) \leq \mathcal{N}_x$. Thus, (4.31) and (4.32) yield

$$\begin{aligned}
& |\mathcal{L}_1 \widetilde{\mathbf{X}}_{L_1}(x) - \mathcal{L}_1(\mathbf{X}_{L_1})_{\mathcal{N}_x}| \\
& \leq C \left(\varepsilon_1 \psi_2 \bar{h}^2 + \nu \left\| p_{11}^{n+1/2} \right\| \psi_1 \bar{h}^3 + \left\| \mathfrak{R}_1^{n+1/2} \right\| \psi_0 \bar{h}^4 \right) (\nu^4 \varepsilon_1^{-4} + \varepsilon_2^{-2}).
\end{aligned} \tag{4.33}$$

Using the suitable barrier functions, then we have

$$\begin{aligned}
& |\mathcal{L}_1 \widetilde{\mathbf{X}}_{L_1}(x) - \mathcal{L}_1(\mathbf{X}_{L_1})_{\mathcal{N}_x}| \leq C \mathcal{N}_x^{-2} (\ln \mathcal{N}_x)^2, \\
& |\mathcal{L}_2 \widetilde{\mathbf{X}}_{L_1}(x) - \mathcal{L}_2(\mathbf{X}_{L_1})_{\mathcal{N}_x}| \leq C \\
& \quad \left(\varepsilon_2 \psi_2 \bar{h}^2 + \nu \left\| p_{22}^{n+1/2} \right\| \psi_1 \bar{h}^3 + \left\| \mathfrak{R}_2^{n+1/2} \right\| \psi_0 \bar{h}^4 \right) (\varepsilon_2^{-1} \varepsilon_1^{-2} \nu + \varepsilon_2^{-3}).
\end{aligned} \tag{4.34}$$

Using the suitable barrier functions, then we have

$$|\mathcal{L}_2 \widetilde{\mathbf{X}}_{L_1}(x) - \mathcal{L}_2(\mathbf{X}_{L_1})_{\mathcal{N}_x}| \leq C \mathcal{N}_x^{-2} (\ln \mathcal{N}_x)^2. \tag{4.35}$$

If $x_m \in (\tau_1, \tau_2]$ or $(1 - \tau_2, 1 - \tau_1)$, $\bar{h} \leq C \mathcal{N}_x^{-2} \tau_2 \leq C \mathcal{N}_x^{-2} (\ln \mathcal{N}_x)^2 \sqrt{\varepsilon_2}$, then we have

$$|\mathcal{L}_1 \widetilde{\mathbf{X}}_{L_1}(x) - \mathcal{L}_1(\mathbf{X}_{L_1})_{\mathcal{N}_x}| \leq C \mathcal{N}_x^{-2} (\ln \mathcal{N}_x)^2 \sqrt{\varepsilon_2} (\varepsilon_1^{-2} \phi_{L_1}(x) + \varepsilon_2^{-2} \phi_{L_2}(x)),$$

and

$$|\mathcal{L}_2 \widetilde{\mathbf{X}}_{L_1}(x) - \mathcal{L}_2(\mathbf{X}_{L_1})_{\mathcal{N}_x}| \leq C \mathcal{N}_x^{-2} (\ln \mathcal{N}_x)^2 \sqrt{\varepsilon_2} (\varepsilon_1^{-2} \phi_{L_1}(x) + \varepsilon_2^{-2} \phi_{L_2}(x)).$$

Using the suitable barrier functions, then we have

$$|\mathcal{L}_1 \widetilde{\mathbf{X}}_{L_1}(x) - \mathcal{L}_1(\mathbf{X}_{L_1})_{\mathcal{N}_x}| \leq C \mathcal{N}_x^{-2} (\ln \mathcal{N}_x)^2,$$

and also

$$|\mathcal{L}_2 \widetilde{\mathbf{X}}_{L_1}(x) - \mathcal{L}_2(\mathbf{X}_{L_1})_{\mathcal{N}_x}| \leq C \mathcal{N}_x^{-2} (\ln \mathcal{N}_x)^2.$$

So, we can obtain

$$|\mathcal{L}^{\mathcal{N}_x} \mathcal{X}_{\mathbf{r}}^{n+1} - \mathcal{L}^{\mathcal{N}_x}(\mathbf{X})_{r_{\mathcal{N}_x}}| \leq C \mathcal{N}_x^{-2} (\ln \mathcal{N}_x)^2. \quad (4.36)$$

When $x_m \in [\tau_2, 1 - \tau_2]$, we can obtain the required bounds by using a method similar to that used in the corresponding intervals of the previous cases. So, for all $0 \leq x_m \leq \mathcal{N}_x$, we have

$$|\mathcal{L}^{\mathcal{N}_x} \mathcal{X}_{\mathbf{L}}^{n+1} - \mathcal{L}^{\mathcal{N}_x}(\mathbf{X})_{L_{\mathcal{N}_x}}| \leq C \mathcal{N}_x^{-2} (\ln \mathcal{N}_x)^2, \quad (4.37)$$

which is the required result for the left layer component $\tilde{\mathbf{X}}_L^{n+1}(x)$.

By following the similar approach, we can prove the parameter uniform error estimates for the component $\tilde{\mathbf{X}}_R^{n+1}(x)$ for this case, obtaining

$$|\mathcal{L}^{\mathcal{N}_x} \mathcal{X}_{\mathbf{R}}^{n+1} - \mathcal{L}^{\mathcal{N}_x}(\mathbf{X})_{R_{\mathcal{N}_x}}| \leq C \mathcal{N}_x^{-2} (\ln \mathcal{N}_x)^2. \quad (4.38)$$

Hence, by combining 4.11, 4.20, 4.21, 4.29, 4.30, 4.37, 4.38, it follows

$$|\mathcal{L}^{\mathcal{N}_x} \tilde{\mathbf{X}}(x_m) - \mathcal{L}^{\mathcal{N}_x} \mathbf{X}_{\mathcal{N}_x}| \leq C \mathcal{N}_x^{-2} (\ln \mathcal{N}_x)^2, \quad 0 \leq n \leq \mathcal{N}_x, \text{ for all the three cases.} \quad (4.39)$$

$$|\mathcal{L}^{\mathcal{N}_x} \mathcal{X}^{n+1} - \mathcal{L}^{\mathcal{N}_x} \mathbf{X}_{\mathcal{N}_x}| = |g(x_m) - \mathcal{L} \mathbf{X}_{\mathcal{N}_x}| \leq C \mathcal{N}_x^{-2} (\ln \mathcal{N}_x)^2. \quad (4.40)$$

Now, for all cases, let $\tilde{\mathbf{L}} \mathbf{X}_{\mathcal{N}_x}(x) = \tilde{g}(x_m)$, $\mathbf{X}_{\mathcal{N}_x}(x_0) = \mathbf{l}_1(s_{n+1})$, $\mathbf{X}_{\mathcal{N}_x}(x_{\mathcal{N}_x}) = \mathbf{m}_1(s_{n+1})$, which results in the linear system

$$\mathcal{A} \tilde{\mathbf{W}}^{n+1} = \tilde{\mathcal{B}}.$$

Next, it follows

$$\mathcal{A}(\mathbf{W}^{n+1} - \tilde{\mathbf{W}}^{n+1}) = \mathcal{B} - \tilde{\mathcal{B}}, \quad (4.41)$$

where

$$\begin{aligned} \mathbf{W}^{n+1} - \tilde{\mathbf{W}}^{n+1} &= (W_{0;1}^{n+1} - \tilde{W}_{0;1}^{n+1}, W_1^{n+1}; 1 - \tilde{W}_1^{n+1}; 1, \dots, W_{\mathcal{N}_x;1}^{n+1} \\ &\quad - \tilde{W}_{\mathcal{N}_x;1}^{n+1}, W_{0;2}^{n+1} - \tilde{W}_{0;2}^{n+1}, \dots, W_{\mathcal{N}_x;2}^{n+1} - \tilde{W}_{\mathcal{N}_x;2}^{n+1})^T, \\ \mathcal{B} - \tilde{\mathcal{B}} &= (g_1(x_0) - \tilde{g}_1(x_0), g_1(x_1) - \tilde{g}_1(x_1), \dots, g_1(x_{\mathcal{N}_x}) \\ &\quad - \tilde{g}_1(x_{\mathcal{N}_x}), g_2(x_0) - \tilde{g}_2(x_0), \dots, g_2(x_{\mathcal{N}_x}) - \tilde{g}_2(x_{\mathcal{N}_x}))^T. \end{aligned}$$

Thus, employing (4.40), we get

$$\|\mathcal{B} - \tilde{\mathcal{B}}\| \leq C \mathcal{N}_x^{-2} (\ln \mathcal{N}_x)^2. \quad (4.42)$$

Following to [30], in a similar way that in [20], we can prove that it holds

$$\|\mathcal{A}^{-1}\|_{\infty} \leq C.$$

Then, from (4.41) and (4.42) we can deduce that it holds

$$\|\mathbf{W}^{n+1} - \widetilde{\mathbf{W}}^{n+1}\| \leq \|\mathcal{A}^{-1}\| \|\mathcal{B} - \widetilde{\mathcal{B}}\| \leq C \mathcal{N}_x^{-2} (\ln \mathcal{N}_x)^2. \quad (4.43)$$

From boundary conditions, we get

$$|W_{-1}^{n+1} - \widetilde{W}_{-1}^{n+1}| \leq C \mathcal{N}_x^{-2} (\ln \mathcal{N}_x)^2,$$

and

$$|W_{\mathcal{N}_x+1}^{n+1} - \widetilde{W}_{\mathcal{N}_x+1}^{n+1}| \leq C \mathcal{N}_x^{-2} (\ln \mathcal{N}_x)^2,$$

and thus

$$\max_{-1 \leq m \leq \mathcal{N}_x+1} |W_m^{n+1} - \widetilde{W}_m^{n+1}| \leq C \mathcal{N}_x^{-2} (\ln \mathcal{N}_x)^2.$$

Hence, we have

$$\begin{aligned} |\mathcal{X}^{n+1} - \mathbf{X}_{\mathcal{N}_x}(x)| &\leq \max_{-1 \leq m \leq \mathcal{N}_x+1} |W_m^{n+1} - \widetilde{W}_m^{n+1}| \\ &\quad + \left| \sum_{m=-1}^{\mathcal{N}_x+1} |\mathcal{D}_m(x)| \right| \leq C \mathcal{N}_x^{-2} (\ln \mathcal{N}_x)^2, \end{aligned}$$

which provides

$$\max_{0 \leq m \leq \mathcal{N}_x} |\mathcal{X}^{n+1} - \mathbf{X}_{\mathcal{N}_x}(x)| \leq C \mathcal{N}_x^{-2} (\ln \mathcal{N}_x)^2.$$

Thus, using the triangle inequality leads to

$$\sup_{0 < \varepsilon_1, \varepsilon_2, \mu \leq 1} \|\mathcal{X}^{n+1} - \widetilde{\mathbf{X}}^{n+1}\| \leq C \mathcal{N}_x^{-2} (\ln \mathcal{N}_x)^2,$$

which is the required result. □

Now, we split the global error at the time t_n in the form

$$[\mathbf{X}(s_n)]_{\Omega_s^{\mathcal{N}_s}} - \widetilde{\mathbf{X}}^n = ([\mathbf{X}(s_n)]_{\Omega_s^{\mathcal{N}_s}} - \mathcal{X}^n) + (\mathcal{X}^n - \widetilde{\mathbf{X}}^n).$$

Then, using Theorems 3.1 and 4.3, we deduce that the fully discrete scheme is a uniformly convergent method, which has second order in time variable and almost second order in spatial variable.

5 Numerical experiments

In this section, we show the numerical results obtained by using our numerical algorithm, for some different test problems of type (1.1). The first example is given by

Example 5.1

$$\begin{cases} \frac{\partial X_1}{\partial s} - \varepsilon_1 \frac{\partial^2 X_1}{\partial x^2} - 7\nu \frac{\partial X_1}{\partial x} + (5+x)X_1 - 3X_2 = -X_1(x, s-0.5) + s^3(1-s), \\ \frac{\partial X_2}{\partial s} - \varepsilon_2 \frac{\partial^2 X_2}{\partial x^2} - 7\nu \frac{\partial X_2}{\partial x} - 2X_1 + (5+e^x)X_2 = -X_1(x, s-0.5) + x^2(1-x)^2, \\ X_1(x, s) = 0, \quad X_2(x, s) = 0, \quad (x, s) \in \mathcal{M}_b \\ X_1(0, s) = 0, \quad X_1(1, s) = 0, \quad X_2(0, s) = 0, \quad X_2(1, s) = 0, \quad s \in [0, 1]. \end{cases}$$

Figures 1, 2, 3 and 4 display the numerical solution obtained for a particular choice of the value of the diffusion, convection and discretization parameters; from them, we clearly observe the boundary layers at both end points of the spatial domain.

The exact solution of this problem is unknown; then, to approximate the maximum errors, the double mesh approach (see [6]) is used. Then, we calculate

$$E_{k, \varepsilon_1, \varepsilon_2, \nu}^{\mathcal{N}_x, \mathcal{N}_s} = \max_{\substack{0 \leq m \leq \mathcal{N}_x \\ 0 \leq n \leq \mathcal{N}_s}} \left(|\tilde{X}_k(x_{2m-1}, s_{2n-1}) - \tilde{X}_k(x_m, s_n)| \right), \quad k = 1, 2,$$

where \tilde{X}_k , $k = 1, 2$, are the components of the solution of a mesh which have the original grid points and its midpoints for both variables. From these values. We calculate the approximated orders of convergence, in an usual way, by

$$R_{k, \varepsilon_1, \varepsilon_2, \nu}^{\mathcal{N}_x, \mathcal{N}_s} = \log_2 \left(E_{k, \varepsilon_1, \varepsilon_2, \nu}^{\mathcal{N}_x, \mathcal{N}_s} / E_{k, \varepsilon_1, \varepsilon_2, \nu}^{2\mathcal{N}_x, 2\mathcal{N}_s} \right), \quad k = 1, 2.$$

Moreover, we calculate the component-wise uniform maximum point wise errors, by using $E_k^{\mathcal{N}_x, \mathcal{N}_s}$, $k = 1, 2$, and from them, the uniform orders of convergence $R_k^{\mathcal{N}_x, \mathcal{N}_s}$, $k = 1, 2$, as follows

$$E_k^{\mathcal{N}_x, \mathcal{N}_s} = \max_{\varepsilon_1, \varepsilon_2, \nu} E_{k, \varepsilon_1, \varepsilon_2, \nu}^{\mathcal{N}_x, \mathcal{N}_s}, \quad R_k^{\mathcal{N}_x, \mathcal{N}_s} = \frac{\log(E_k^{\mathcal{N}_x, \mathcal{N}_s} / E_k^{2\mathcal{N}_x, 2\mathcal{N}_s})}{\log 2}, \quad k = 1, 2.$$

We use the Block Thomas Algorithm with each block of 2×2 matrix to solve the linear systems resulting when we solve systems with two equations (Examples 1 and 2) and each block of 3×3 matrix to solve the linear systems resulting when we solve systems with three equations (Example 3). Moreover, each table also shows the CPU time (in seconds) taken for all values of the diffusion parameters at each column with

N_x and N_s fixed. We can see from this table that the CPU time is small and is unaffected by the values of the convection and the diffusion parameters.

Tables 1, 2 and 3 show the numerical results obtained by our algorithm for each one of the three different cases, respectively, depending on the value and the ratio between the diffusion and the convection parameters. From them, we clearly see the almost second order of uniform convergence of the numerical method, in agreement with the theoretical results.

Due that Tables 1, 2 and 3 show almost second order of uniform convergence, we can conclude that, in this example, the errors associated to the spatial discretization dominate in the global errors of the numerical method. To see numerically the second order of the time discretization, in agreement with Remark 3.2, we include a new table. Table 4 shows the numerical results obtained when the discretization parameter N_s is multiplied by 2 but the discretization parameter N_x is multiplied by 4; from this table, we clearly observe the second order of uniform convergence of the time discretization according our theoretical result. Here, we only show the results for the case when $\alpha \nu^2 \geq \eta \varepsilon_2$ holds; similar results are obtained for the other two cases, $\alpha \nu^2 \leq \eta \varepsilon_1$ and $\eta \varepsilon_1 < \alpha \nu^2 < \eta \varepsilon_2$.

The second test problem that we consider is given by

Example 5.2

$$\begin{cases} \frac{\partial X_1}{\partial s} - \varepsilon_1 \frac{\partial^2 X_1}{\partial x^2} - \left(1 + x^2 + \frac{\sin(\pi x)}{2}\right) \nu \frac{\partial X_1}{\partial x} + (2x(1+s)^2) X_1 - 2X_2 = -X_1(x, s-0.4) + \exp(x)s(1-s), \\ \frac{\partial X_2}{\partial s} - \varepsilon_2 \frac{\partial^2 X_2}{\partial x^2} - (1+2x)\nu \frac{\partial X_2}{\partial x} - X_1 + (10x+1)s^2(1-s)^2 X_2 = -X_1(x, s-0.4) + x^2(1-x)^2, \\ X_1(x, s) = 0, X_2(x, s) = 0, (x, s) \in \mathcal{M}_b \\ X_1(0, s) = \sin(\pi x), X_1(1, s) = 0, X_2(0, s) = \sin(\pi x), X_2(1, s) = 0, s \in [0, 1]. \end{cases}$$

In this case, again the exact solution is unknown; then, we use the double mesh principle to approximate the maximum errors and the numerical orders of convergence obtained by using our algorithm.

Figures 5, 6, 7 and 8 display the numerical solution obtained for a particular choice of the value of the diffusion, convection and discretization parameters; from them, again the boundary layers at both end points of the spatial domain are observed.

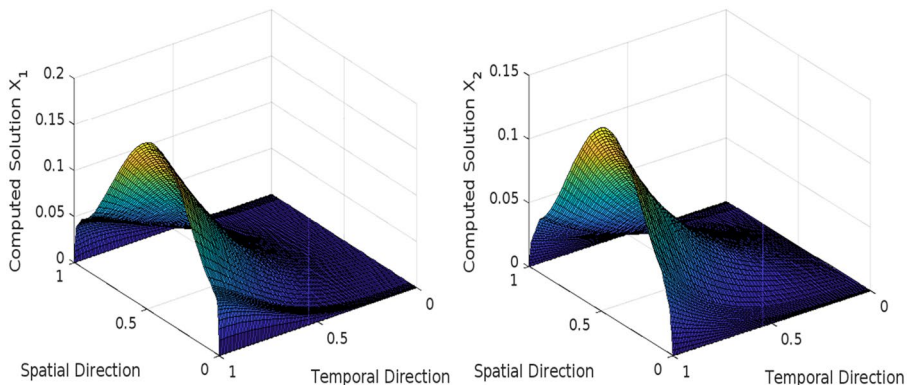


Fig. 1 When $\varepsilon_1 = 4^{-2}2^{-10}$, $\varepsilon_2 = 2^{-2}2^{-10}$, $\nu^2 = 5^{-4}2^{-10}$, $\mathcal{N}_x = \mathcal{N}_s = 128$ for example 5.1

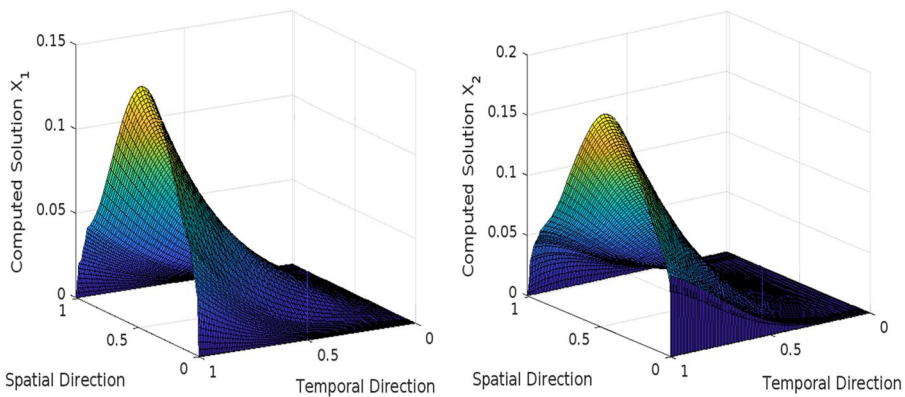


Fig. 2 When $\varepsilon_1 = 5^{-2}2^{-10}$, $\varepsilon_2 = 3^{-2}2^{-10}$, $\nu^2 = 2^{-2}2^{-10}$, $\mathcal{N}_x = \mathcal{N}_s = 128$ for example 5.1

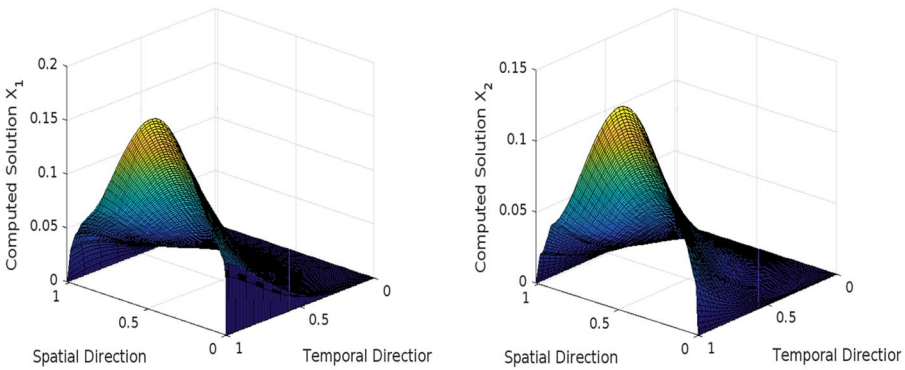


Fig. 3 When $\varepsilon_1 = 6^{-2}2^{-10}$, $\varepsilon_2 = 2^{-2}2^{-10}$, $\nu^2 = 4^{-2}2^{-10}$, $\mathcal{N}_x = \mathcal{N}_s = 128$ for example 5.1

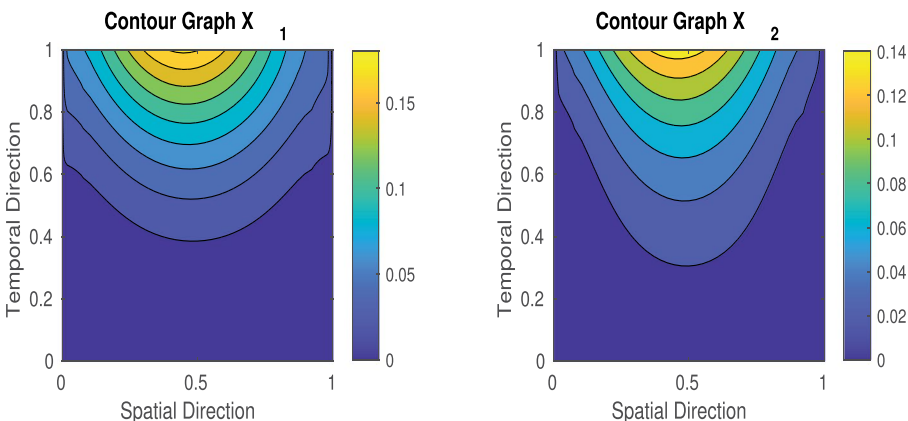


Fig. 4 Contour plots when $\varepsilon_1 = 4^{-2}2^{-10}$, $\varepsilon_2 = 2^{-2}2^{-10}$, $\nu^2 = 5^{-4}2^{-10}$, $\mathcal{N}_x = \mathcal{N}_s = 128$ for example 5.1

Table 1 For example 5.1 maximum point-wise errors and orders of convergence when $\alpha, \nu^2 \leq \eta \varepsilon_1$.

δ	$\varepsilon_1 = 4^{-2}\delta, \varepsilon_2 = 2^{-2}\delta, \nu^2 = 5^{-4}\delta$	$\mathcal{N}_s = \mathcal{N}_x = 32$	$\mathcal{N}_s = \mathcal{N}_x = 64$	$\mathcal{N}_s = \mathcal{N}_x = 128$	$\mathcal{N}_s = \mathcal{N}_x = 256$	$\mathcal{N}_s = \mathcal{N}_x = 512$
2 ⁰	7.5908E - 4	1.9209E - 4	4.7317E - 5	1.1755E - 5	2.8466E - 6	
2 ⁻²	2.3912E - 3	6.4720E - 4	1.6053E - 4	4.0112E - 5	1.0102E - 5	
2 ⁻⁴	4.6966E - 3	1.1152E - 3	2.6373E - 4	6.5884E - 5	1.5520E - 5	
2 ⁻⁶	9.7316E - 3	3.6453E - 3	9.4741E - 4	2.1874E - 4	5.4218E - 5	
2 ⁻⁸	1.5020E - 2	5.6675E - 3	1.6169E - 3	4.1871E - 4	1.0270E - 4	
2 ⁻¹⁰	1.5120E - 2	5.6770E - 3	1.6265E - 3	4.1970E - 4	1.0380E - 4	
2 ⁻¹²	1.5170E - 2	5.6810E - 3	1.6298E - 3	4.1997E - 4	1.0415E - 4	
2 ⁻¹⁴	1.5192E - 2	5.6831E - 3	1.6318E - 3	4.2019E - 4	1.0432E - 4	
2 ⁻¹⁶	1.5199E - 2	5.6838E - 3	1.6323E - 3	4.2022E - 4	1.0435E - 4	
2 ⁻¹⁸	1.5201E - 2	5.6840E - 3	1.6326E - 3	4.2024E - 4	1.0437E - 4	
2 ⁻²⁰	1.5202E - 2	5.6841E - 3	1.6326E - 3	4.2024E - 4	1.0438E - 4	
2 ⁻²²	1.5202E - 2	5.6841E - 3	1.6326E - 3	4.2024E - 4	1.0438E - 4	
$E_1^{\mathcal{N}_s, \mathcal{N}_x}$	1.5202E - 2	5.6841E - 3	1.6326E - 3	4.2024E - 4	1.0438E - 4	
$R_1^{\mathcal{N}_s, \mathcal{N}_x}$	1.4193	1.7998	1.9579	2.0094		
CPU time (seconds)	0.0659	0.0938	0.4609	0.0320		

Table 2 For example 5.1 maximum point-wise errors and orders of convergence when $\eta \varepsilon_1 < \alpha \nu^2 < \eta \varepsilon_2$.

δ	$\mathcal{N}_s = \mathcal{N}_x = 32$	$\mathcal{N}_s = \mathcal{N}_x = 64$	$\mathcal{N}_s = \mathcal{N}_x = 128$	$\mathcal{N}_s = \mathcal{N}_x = 256$	$\mathcal{N}_s = \mathcal{N}_x = 512$
2 ⁰	1.8245E-2	6.1386E-3	1.4765E-3	3.3007E-4	7.9466E-5
2 ⁻²	6.4667E-2	2.0481E-2	5.1273E-3	1.0132E-3	2.5102E-4
2 ⁻⁴	8.4767E-2	3.0281E-2	8.6373E-3	2.1384E-3	4.9850E-4
2 ⁻⁶	9.9326E-2	3.1403E-2	9.8741E-3	2.5874E-3	6.0213E-4
2 ⁻⁸	9.9786E-2	3.1813E-2	9.9640E-3	2.6281E-3	6.0710E-4
2 ⁻¹⁰	9.9969E-2	3.2017E-2	9.9820E-3	2.6480E-3	6.0910E-4
2 ⁻¹²	9.1083E-2	3.2115E-2	9.9910E-3	2.6575E-3	6.1013E-4
2 ⁻¹⁴	9.1144E-2	3.2155E-2	9.9963E-3	2.6620E-3	6.1060E-4
2 ⁻¹⁶	9.138E-2	3.2176E-2	9.9980E-3	2.6638E-3	6.1076E-4
2 ⁻¹⁸	9.142E-2	3.2185E-2	9.9991E-3	2.6646E-3	6.1094E-4
2 ⁻²⁰	9.144E-2	3.2187E-2	9.9992E-3	2.6647E-3	6.1096E-4
2 ⁻²²	9.144E-2	3.2187E-2	9.9992E-3	2.6647E-3	6.1096E-4
$E_1^{\mathcal{N}_s, \mathcal{N}_x}$	9.144E-2	3.2187E-2	9.9992E-3	2.6647E-3	6.1096E-4
$R_1^{\mathcal{N}_s, \mathcal{N}_x}$	1.5063	1.6866	1.9078	2.1248	
CPU time (seconds)	0.0731	0.0952	0.1132	0.4642	0.9796

Table 3 For example 5.1 maximum point-wise errors and orders of convergence when $\alpha \nu^2 \geq \eta \varepsilon_2$.

δ	$\varepsilon_1 = 5^{-2}\delta, \varepsilon_2 = 3^{-2}\delta, \nu^2 = 2^{-2}\delta$	$\mathcal{N}_s = \mathcal{N}_x = 32$	$\mathcal{N}_s = \mathcal{N}_x = 64$	$\mathcal{N}_s = \mathcal{N}_x = 128$	$\mathcal{N}_s = \mathcal{N}_x = 256$	$\mathcal{N}_s = \mathcal{N}_x = 512$
2^{-20}		$2.2065E-2$	$9.2667E-3$	$2.8702E-3$	$7.6183E-4$	$2.0106E-4$
2^{-18}		$5.9586E-2$	$1.8544E-2$	$5.2016E-3$	$1.3792E-3$	$3.0712E-4$
2^{-16}		$7.9280E-2$	$2.4563E-2$	$6.6382E-3$	$1.7304E-3$	$4.1520E-4$
2^{-14}		$8.7326E-2$	$3.1453E-2$	$7.4860E-3$	$2.1838E-3$	$5.4227E-4$
2^{-12}		$8.7320E-2$	$3.2170E-2$	$7.4660E-3$	$2.2374E-3$	$5.4517E-4$
2^{-10}		$8.9620E-2$	$3.2350E-2$	$7.4842E-3$	$2.2552E-3$	$5.4701E-4$
2^{-8}		$8.9989E-2$	$3.2381E-2$	$7.4874E-3$	$2.2580E-3$	$5.4721E-4$
2^{-14}		$8.9996E-2$	$3.2386E-2$	$7.4878E-3$	$2.2583E-3$	$5.4723E-4$
2^{-16}		$8.9998E-2$	$3.2388E-2$	$7.4880E-3$	$2.2584E-3$	$5.4724E-4$
2^{-18}		$8.9998E-2$	$3.2388E-2$	$7.4880E-3$	$2.2584E-3$	$5.4724E-4$
2^{-20}		$8.9998E-2$	$3.2388E-2$	$7.4880E-3$	$2.2584E-3$	$5.4724E-4$
2^{-22}		$8.9998E-2$	$3.2388E-2$	$7.4880E-3$	$2.2584E-3$	$5.4724E-4$
$E_1^{\mathcal{N}_s, \mathcal{N}_x}$		$8.9998E-2$	$3.2388E-2$	$7.4880E-3$	$2.2584E-3$	$5.4724E-4$
$R_1^{\mathcal{N}_s, \mathcal{N}_x}$		1.4193	1.4744	1.7293	2.0451	
CPU time (seconds)		0.0641	0.0853	0.1032	0.5293	0.9912

Tables 5, 6 and 7 show the numerical results obtained for this example; from them, the almost second order of uniform convergence of the numerical method can be deduced.

To see that our method can be extended to systems with a bigger number of equations, we consider a new example, which is given by

Example 5.3

$$\begin{cases} \frac{\partial X_1}{\partial s} - \varepsilon_1 \frac{\partial^2 X_1}{\partial x^2} - 5\nu \frac{\partial X_1}{\partial x} + (4+x)X_1 - 2X_2 - X_3 = -X_1(x, s-0.5) + s^2(1-s), \\ \frac{\partial X_2}{\partial s} - \varepsilon_2 \frac{\partial^2 X_2}{\partial x^2} - 6\nu \frac{\partial X_2}{\partial x} - 2X_1 + (4+\sin x)X_2 - X_3 = -X_1(x, s-0.5) + x(1-x)^2, \\ \frac{\partial X_3}{\partial s} - \varepsilon_3 \frac{\partial^2 X_3}{\partial x^2} - 7\nu \frac{\partial X_3}{\partial x} - X_1 - X_2 + (4+\cos x)X_3 = -X_1(x, s-0.5) + e^x(1-x), \\ X_1(x, s) = 0, X_2(x, s) = 0, X_3(x, s) = 0, (x, s) \in \mathcal{M}_b, \\ X_1(0, s) = X_1(1, s) = 0, X_2(0, s) = X_2(1, s) = 0, X_3(0, s) = X_3(1, s) = 0, s \in [0, 1]. \end{cases}$$

Similarly to the case of two equations, we assume that $0 < \varepsilon_1 \leq \varepsilon_2 \leq \varepsilon_3 \leq 1$ and $0 \leq \nu \leq 1$. To discretize this new system, we use the same discretization as before, i.e., the Crank-Nicolson on a uniform mesh to discretize in time and the \mathcal{B} -splines to discretize in space on an adequate Shishkin mesh. The only new question is the definition of the Shishkin mesh. To do that, now we distinguish four different cases.

Similarly to the case of two equations, we assume that $0 < \varepsilon_1 \leq \varepsilon_2 \leq \varepsilon_3 \leq 1$ and $0 \leq \nu \leq 1$. To discretize this new system, we use the same discretization as before, i.e., the Crank-Nicolson on a uniform mesh to discretize in time and the \mathcal{B} -splines to discretize in space on an adequate Shishkin mesh. The only new question is the definition of the Shishkin mesh. To do that, now we distinguish four different cases.

Case 1: If $\alpha \nu^2 \leq \eta \varepsilon_1$, we subdivide the unit interval into seven subintervals each as

$$[0, 1] = [0, \tau_1] \cup [\tau_1, \tau_2] \cup [\tau_2, \tau_3] \cup [\tau_3, 1 - \tau_3] \cup [1 - \tau_3, 1 - \tau_2] \cup [1 - \tau_2, 1 - \tau_1] \cup [1 - \tau_1, 1],$$

where the transition points τ_1, τ_2 and τ_3 are defined by

$$\tau_1 = \min \left\{ \frac{\tau_2}{2}, \sqrt{\frac{\varepsilon_1}{\alpha \eta}} \ln N_x \right\}, \tau_2 = \min \left\{ \frac{\tau_3}{2}, \sqrt{\frac{\varepsilon_2}{\alpha \eta}} \ln N_x \right\}, \tau_3 = \min \left\{ \frac{1}{8}, \sqrt{\frac{\varepsilon_3}{\alpha \eta}} \ln N_x \right\}. \quad (5.1)$$

There, with N_x a positive integer multiple of 12, we take are $N_x/12 + 1$ uniformly spaced grid points on each of the subintervals $[0, \tau_1], [\tau_1, \tau_2], [\tau_2, \tau_3], [1 - \tau_3, 1 - \tau_2], [1 - \tau_2, 1 - \tau_1]$, and $[1 - \tau_1, 1]$. On the remaining subinterval $[\tau_3, 1 - \tau_3]$, there are $N_x/2 + 1$ uniformly spaced grid points.

Case 2: If $\alpha \nu^2 \geq \eta \varepsilon_3$, then, the unit interval is divided into five subintervals each by the appropriate fitted non-uniform Shishkin mesh each as

$$[0, 1] = [0, \tau_1] \cup [\tau_1, \tau_2] \cup [\tau_2, \tau_3] \cup [\tau_3, 1 - \sigma_1] \cup [1 - \sigma_1, 1],$$

where now the transition points τ_1, τ_2, τ_3 and σ_1 are defined by

Table 4 For example 5.1 maximum point-wise errors and orders of convergence when $\alpha, \nu^2 \geq \eta \varepsilon_2$.

δ	$\varepsilon_1 = 5^{-2}\delta, \varepsilon_2 = 3^{-2}\delta, \nu^2 = 2^{-2}\delta$	$\mathcal{N}_s = 16, N_x = 16$	$\mathcal{N}_s = 32, N_x = 64$	$\mathcal{N}_s = 64, N_x = 128$	$\mathcal{N}_s = 128, N_x = 256$
2 ⁰	6.8964E - 2	1.8634E - 2	4.8614E - 3	1.2184E - 3	
2 ⁻²	8.9359E - 2	2.4217E - 2	6.2076E - 3	1.6254E - 3	
2 ⁻⁴	9.5237E - 2	2.5723E - 2	6.6012E - 3	1.8304E - 3	
2 ⁻⁶	9.8413E - 2	2.8783E - 2	7.4215E - 3	1.8408E - 3	
2 ⁻⁸	9.8713E - 2	2.8965E - 2	7.4515E - 3	1.8413E - 3	
2 ⁻¹⁰	9.8987E - 2	2.9062E - 2	7.4717E - 3	1.8517E - 3	
2 ⁻¹²	9.8998E - 2	3.2381E - 2	7.4723E - 3	1.8521E - 3	
2 ⁻¹⁴	9.9004E - 2	2.9082E - 2	7.4729E - 3	1.8524E - 3	
2 ⁻¹⁶	9.9006E - 2	2.9083E - 2	7.4731E - 3	1.8525E - 3	
2 ⁻¹⁸	9.9006E - 2	2.9083E - 2	7.4731E - 3	1.8525E - 3	
2 ⁻²⁰	9.9006E - 2	2.9083E - 2	7.4731E - 3	1.8525E - 3	
2 ⁻²²	9.9006E - 2	2.9083E - 2	7.4731E - 3	1.8525E - 3	
$E_1^{\mathcal{N}_s, \mathcal{N}_x}$	9.9006E - 2	2.9083E - 2	7.4731E - 3	1.8525E - 3	
$R_1^{\mathcal{N}_s, \mathcal{N}_x}$	1.7673	1.9604	2.0122	2.032	1.5833
CPU time (seconds)	0.0441	0.0658			

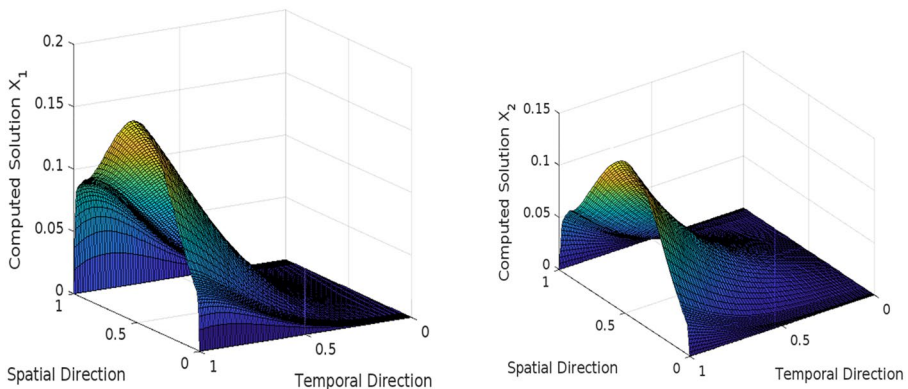


Fig. 5 When $\varepsilon_1 = 4^{-2}2^{-10}$, $\varepsilon_2 = 2^{-2}2^{-10}$, $\nu^2 = 5^{-4}2^{-10}$, $\mathcal{N}_x = \mathcal{N}_s = 128$ for example 5.2

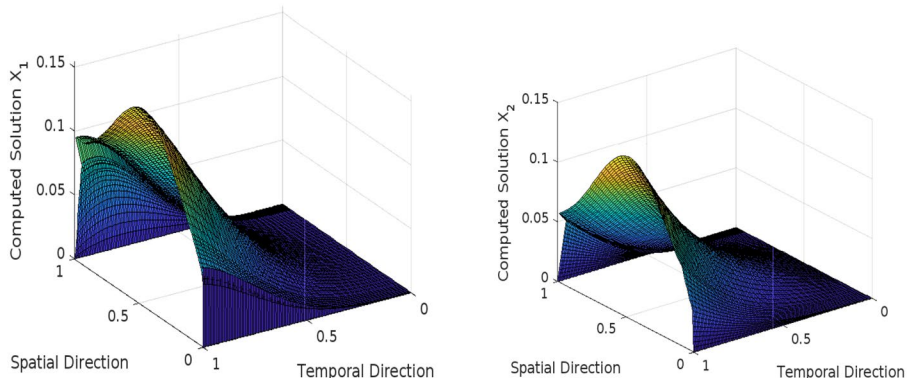


Fig. 6 When $\varepsilon_1 = 6^{-2}2^{-10}$, $\varepsilon_2 = 2^{-2}2^{-10}$, $\nu^2 = 4^{-2}2^{-10}$, $\mathcal{N}_x = \mathcal{N}_s = 128$ for example 5.2

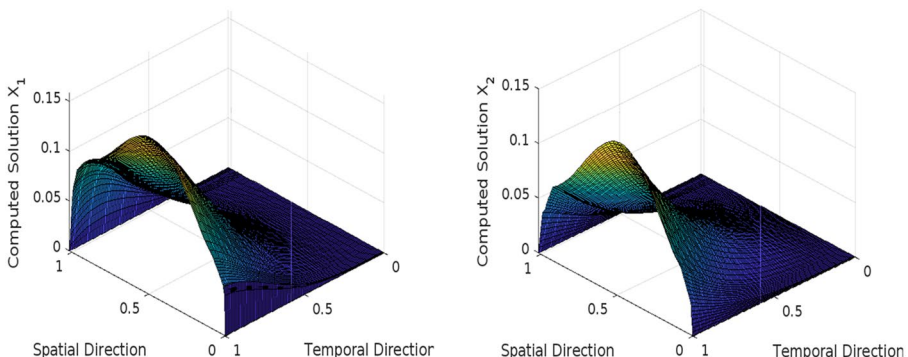


Fig. 7 When $\varepsilon_1 = 5^{-2}2^{-10}$, $\varepsilon_2 = 3^{-2}2^{-10}$, $\nu^2 = 2^{-2}2^{-10}$, $\mathcal{N}_x = \mathcal{N}_s = 128$ for example 5.2

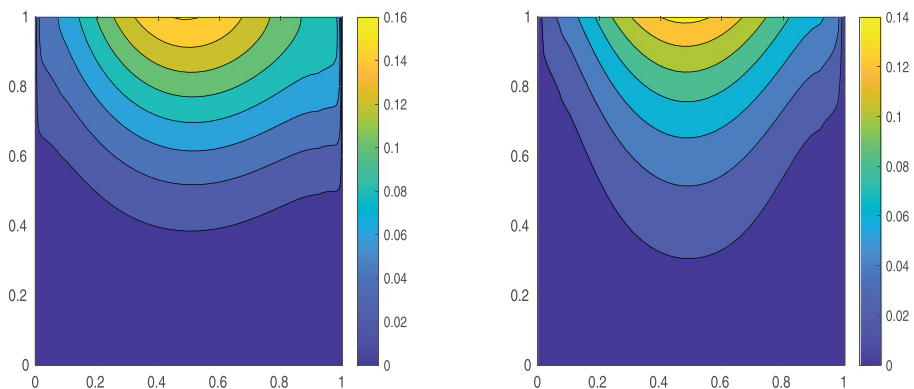


Fig. 8 Contour plots when $\varepsilon_1 = 4^{-2}2^{-10}$, $\varepsilon_2 = 2^{-2}2^{-10}$, $\nu^2 = 5^{-4}2^{-10}$, $\mathcal{N}_x = \mathcal{N}_s = 128$ for example 5.2

$$\begin{aligned}\tau_1 &= \min \left\{ \frac{\tau_2}{2}, \frac{\varepsilon_1}{\nu\alpha} \ln N_x \right\}, \quad \tau_2 = \min \left\{ \frac{\tau_3}{2}, \frac{\varepsilon_2}{\nu\alpha} \ln N_x \right\}, \\ \tau_3 &= \min \left\{ \frac{1}{8}, \frac{\varepsilon_3}{\nu\alpha} \ln N_x \right\}, \quad \sigma_1 = \min \left\{ \frac{1}{4}, \frac{\nu}{\eta} \ln N_x \right\}.\end{aligned}$$

There, with N_x a positive integer multiple of 8, we take $N_x/2 + 1$ evenly spaced grid points on the subinterval $[\tau_3, 1 - \sigma_1]$, whereas the remaining subinterval $[0, \tau_1]$, $[\tau_1, \tau_2]$, $[\tau_2, \tau_3]$ there are $N_x/8 + 1$ uniformly spaced grid points, and $N_x/4 + 1$ uniformly spaced grid points on the subinterval $[1 - \sigma_1, 1]$.

Case 3: If $\eta \varepsilon_2 < \alpha \nu^2 < \eta \varepsilon_3$, then, the unit interval is divided into six subintervals each by the appropriate fitted non-uniform Shishkin mesh each as

$$[0, 1] = [0, \tau_1] \cup [\tau_1, \tau_2] \cup [\tau_2, \tau_3] \cup [\tau_3, 1 - \tau_3] \cup [1 - \tau_3, 1 - \sigma_1] \cup [1 - \sigma_1, 1],$$

where now the transition points τ_1 , τ_2 , τ_3 and σ_1 are defined by

$$\begin{aligned}\tau_1 &= \min \left\{ \frac{\tau_2}{2}, \frac{\varepsilon_1}{\nu\alpha} \ln N_x \right\}, \quad \tau_2 = \min \left\{ \frac{\tau_3}{2}, \frac{\varepsilon_2}{\nu\alpha} \ln N_x \right\}, \\ \tau_3 &= \min \left\{ \frac{1}{8}, \sqrt{\frac{\varepsilon_3}{\alpha\eta}} \ln N_x \right\}, \quad \sigma_1 = \min \left\{ \frac{1}{8}, \frac{\nu}{\eta} \ln N_x \right\}.\end{aligned}$$

Then, with N_x a positive integer multiple of 8, we take are $3N_x/8 + 1$ evenly spaced grid points on the subinterval $[\tau_3, 1 - \tau_3]$, whereas the remaining subinterval $[0, \tau_1]$, $[\tau_1, \tau_2]$, $[\tau_2, \tau_3]$, $[1 - \tau_3, 1 - \sigma_1]$ and $[1 - \sigma_1, 1]$ there are $N_x/8 + 1$ uniformly spaced grid points.

Case 4: If $\eta \varepsilon_1 < \alpha \nu^2 < \eta \varepsilon_2$, then, the unit interval $[0, 1]$ is divided into six subintervals each by the piecewise uniform Shishkin mesh each as

Table 5 For example 5.2, maximum point-wise errors and orders of convergence when $\alpha \cdot \nu^2 \leq \eta \cdot \varepsilon_1$.

δ	$\varepsilon_1 = 4^{-2}\delta, \varepsilon_2 = 2^{-2}\delta, \nu^2 = 5^{-4}\delta$			$\varepsilon_1 = 4^{-2}\delta, \varepsilon_2 = 2^{-2}\delta, \nu^2 = 5^{-4}\delta$		
	$\mathcal{N}_s = \mathcal{N}_x = 32$	$\mathcal{N}_s = \mathcal{N}_x = 64$	$\mathcal{N}_s = \mathcal{N}_x = 128$	$\mathcal{N}_s = \mathcal{N}_x = 256$	$\mathcal{N}_s = \mathcal{N}_x = 512$	
2 ⁰	1.0340E - 3	2.8815E - 4	7.6725E - 5	1.9725E - 5	4.8423E - 6	
2 ⁻²	1.6970E - 3	4.8277E - 4	1.3243E - 4	3.4176E - 5	8.0152E - 6	
2 ⁻⁴	1.7958E - 3	5.6047E - 4	1.6158E - 4	4.4324E - 5	9.8051E - 6	
2 ⁻⁶	2.8425E - 3	7.6143E - 4	1.9856E - 4	5.1327E - 5	1.2067E - 5	
2 ⁻⁸	2.9667E - 3	7.9341E - 4	2.3057E - 4	5.9312E - 5	1.4017E - 5	
2 ⁻¹⁰	2.9774E - 3	8.2517E - 4	2.3120E - 4	5.9370E - 5	1.4104E - 5	
2 ⁻¹²	2.9897E - 3	8.2607E - 4	2.3137E - 4	5.9448E - 5	1.4184E - 5	
2 ⁻¹⁴	2.9967E - 3	8.2678E - 4	2.3127E - 4	5.9463E - 5	1.4196E - 5	
2 ⁻¹⁶	2.9972E - 3	8.2683E - 4	2.3134E - 4	5.9466E - 5	1.4201E - 5	
2 ⁻¹⁸	2.9974E - 3	8.2685E - 4	2.3135E - 4	5.9467E - 5	1.4202E - 5	
2 ⁻²⁰	2.9974E - 3	8.2685E - 4	2.3135E - 4	5.9467E - 5	1.4202E - 5	
2 ⁻²²	2.9974E - 3	8.2685E - 4	2.3135E - 4	5.9467E - 5	1.4202E - 5	
$E_1^{\mathcal{N}_s, \mathcal{N}_x}$	2.9974E - 3	8.2685E - 4	2.3135E - 4	5.9467E - 5	1.4202E - 5	
$R_1^{\mathcal{N}_s, \mathcal{N}_x}$	1.8580	1.8375	1.9599	2.0660		
CPU time (seconds)	0.0872	0.0992	0.1158	0.8388	1.3052	

Table 6 For example 5.2 maximum point-wise errors and orders of convergence when $\eta \varepsilon_1 < \alpha \nu^2 < \eta \varepsilon_2$.

δ	$\varepsilon_1 = 6^{-2}\delta, \varepsilon_2 = 2^{-2}\delta, \nu^2 = 4^{-2}\delta$			$\varepsilon_1 = 6^{-2}\delta, \varepsilon_2 = 32$			$\varepsilon_1 = 6^{-2}\delta, \varepsilon_2 = 64$			$\varepsilon_1 = 6^{-2}\delta, \varepsilon_2 = 128$			$\varepsilon_1 = 6^{-2}\delta, \varepsilon_2 = 256$		
2 ⁰	2.1884E-2			7.3911E-3			1.7843E-3			3.9840E-4			9.3578E-5		
2 ⁻²	2.4514E-2			8.3157E-3			2.0132E-3			5.0164E-4			1.2420E-4		
2 ⁻⁴	2.7276E-2			8.7984E-3			2.6313E-3			6.5372E-4			1.5820E-4		
2 ⁻⁶	3.1293E-2			9.0930E-3			2.7318E-3			7.0874E-4			1.8921E-4		
2 ⁻⁸	3.6891E-2			1.2372E-2			3.1628E-3			8.1025E-4			2.0230E-4		
2 ⁻¹⁰	4.5782E-2			1.5266E-2			3.8939E-3			9.9518E-4			2.5143E-4		
2 ⁻¹²	4.8712E-2			1.6582E-2			5.2179E-3			1.2518E-3			3.1123E-4		
2 ⁻¹⁴	4.8978E-2			1.6798E-2			5.2398E-3			1.2753E-3			3.1358E-4		
2 ⁻¹⁶	4.8999E-2			1.6816E-2			5.2418E-3			1.2795E-3			3.1379E-4		
2 ⁻¹⁸	4.9012E-2			1.6819E-2			5.2423E-3			1.2798E-3			3.1383E-4		
2 ⁻²⁰	4.9014E-2			1.6821E-2			5.2424E-3			1.2798E-3			3.1384E-4		
2 ⁻²²	4.9014E-2			1.6821E-2			5.2424E-3			1.2798E-3			3.1384E-4		
$E_1^{\mathcal{N}_s, \mathcal{N}_x}$	4.9014E-2			1.6821E-2			5.2424E-3			1.2798E-3			3.1384E-4		
$R_1^{\mathcal{N}_s, \mathcal{N}_x}$	1.5429			1.6820			2.0343			2.0278					
CPU time (seconds)	0.0625			0.0687			0.0874			1.0621			1.1345		

Table 7 For example 5.2 maximum point-wise errors and orders of convergence when $\alpha, \nu^2 \geq \eta \varepsilon_2$.

δ	$\varepsilon_1 = 5^{-2}\delta, \varepsilon_2 = 3^{-2}\delta, \nu^2 = 2^{-2}\delta$	$\mathcal{N}_s = \mathcal{N}_x = 32$	$\mathcal{N}_s = \mathcal{N}_x = 64$	$\mathcal{N}_s = \mathcal{N}_x = 128$	$\mathcal{N}_s = \mathcal{N}_x = 256$	$\mathcal{N}_s = \mathcal{N}_x = 512$
2^0		$3.9191E - 2$	$1.1263E - 2$	$3.1023E - 3$	$7.9513E - 4$	$1.9813E - 4$
2^{-2}		$5.9487E - 2$	$1.7048E - 2$	$4.6017E - 3$	$1.2142E - 3$	$3.1255E - 4$
2^{-4}		$7.0865E - 2$	$2.0263E - 2$	$5.5322E - 3$	$1.5032E - 3$	$3.7230E - 4$
2^{-6}		$8.4942E - 2$	$2.4313E - 2$	$6.7536E - 3$	$1.8252E - 3$	$4.6807E - 4$
2^{-8}		$8.7579E - 2$	$2.5022E - 2$	$6.955E - 3$	$1.8296E - 3$	$4.6912E - 4$
2^{-10}		$8.9593E - 2$	$2.5598E - 2$	$7.1105E - 3$	$1.8711E - 3$	$4.7976E - 4$
2^{-12}		$9.1937E - 2$	$2.6317E - 2$	$7.3108E - 3$	$2.0520E - 3$	$5.2615E - 4$
2^{-14}		$9.1977E - 2$	$2.6345E - 2$	$7.3142E - 3$	$2.0553E - 3$	$5.2643E - 4$
2^{-16}		$9.1979E - 2$	$2.6346E - 2$	$7.3144E - 3$	$2.0554E - 3$	$5.2643E - 4$
2^{-18}		$9.1981E - 2$	$2.6347E - 2$	$7.3144E - 3$	$2.0555E - 3$	$5.2643E - 4$
2^{-20}		$9.1981E - 2$	$2.6347E - 2$	$7.3144E - 3$	$2.0555E - 3$	$5.2643E - 4$
2^{-22}		$9.1981E - 2$	$2.6347E - 2$	$7.3144E - 3$	$2.0555E - 3$	$5.2643E - 4$
$E_1^{\mathcal{N}_s, \mathcal{N}_x}$		$9.1981E - 2$	1.8488	1.8313	1.9652	
$R_1^{\mathcal{N}_s, \mathcal{N}_x}$		1.8037	0.0997	0.4872	0.9215	
CPU time (seconds)		0.0856			1.3305	

$$[0, 1] = [0, \tau_1] \cup [\tau_1, \tau_2] \cup [\tau_2, \tau_3] \cup [\tau_3, 1 - \tau_3] \cup [1 - \tau_3, 1 - \sigma_1] \cup [1 - \sigma_1, 1],$$

where σ_1 and τ_1, τ_2 are the transition points, which are now defined by

$$\begin{aligned}\tau_1 &= \min \left\{ \frac{\tau_2}{2}, \frac{\varepsilon_1}{\nu\alpha} \ln N_x \right\}, \quad \tau_2 = \min \left\{ \frac{\tau_3}{2}, \sqrt{\frac{\varepsilon_2}{\alpha\eta}} \ln N_x \right\}, \\ \tau_3 &= \min \left\{ \frac{1}{8}, \sqrt{\frac{\varepsilon_3}{\alpha\eta}} \ln N_x \right\}, \quad \sigma_1 = \min \left\{ \frac{1}{8}, \frac{\nu}{\eta} \ln N_x \right\}.\end{aligned}$$

Then, with N_x a positive integer multiple of 8, we take are $3N_x/8 + 1$ evenly spaced grid points on the subinterval $[\tau_3, 1 - \tau_3]$, whereas the remaining subinterval $[0, \tau_1]$, $[\tau_1, \tau_2]$, $[\tau_2, \tau_3]$, $[1 - \tau_3, 1 - \sigma_1]$ and $[1 - \sigma_1, 1]$ there are $N_x/8 + 1$ uniformly spaced grid points.

Figures 9, 10, 11 and 12 display the numerical solution obtained for a particular choice of the value of the diffusion, convection and discretization parameters for all the four cases; clearly, the boundary layers at both end points of the spatial domain are observed.

Tables 8, 9, 10 and 11 show the numerical results obtained for this example; from them, the second order of uniform convergence of the numerical method can be deduced. Then, we see that the technique used in this work can be extended to systems with a bigger number of equations; the numerical results show again the efficiency and the order of uniform convergence of the numerical algorithm.

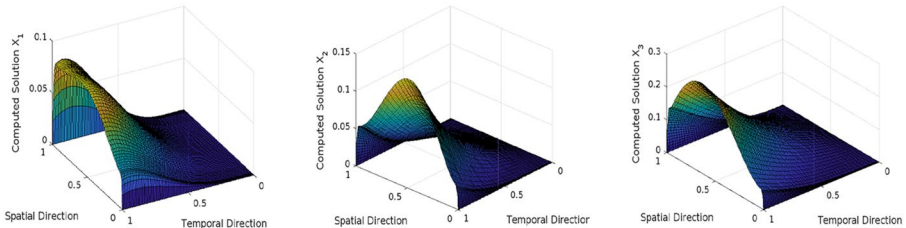


Fig. 9 When $\varepsilon_1 = 4^{-2}2^{-10}$, $\varepsilon_2 = 3^{-2}2^{-10}$, $\varepsilon_3 = 2^{-2}2^{-10}$, $\nu^2 = 5^{-4}2^{-10}$, $\mathcal{N}_x = \mathcal{N}_s = 128$ for example 5.3

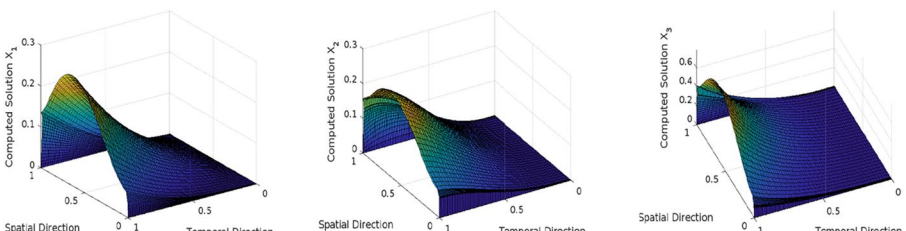


Fig. 10 When $\varepsilon_1 = 5^{-2}2^{-10}$, $\varepsilon_2 = 4^{-2}2^{-10}$, $\varepsilon_3 = 3^{-2}2^{-10}$, $\nu^2 = 2^{-2}2^{-10}$, $\mathcal{N}_x = \mathcal{N}_s = 128$ for example 5.3

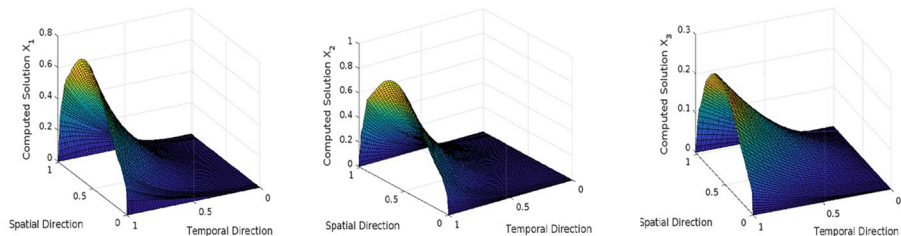


Fig. 11 When $\varepsilon_1 = 8^{-2}2^{-10}$, $\varepsilon_2 = 6^{-2}2^{-10}$, $\varepsilon_3 = 2^{-2}2^{-10}$, $\nu^2 = 4^{-2}2^{-10}$, $\mathcal{N}_x = \mathcal{N}_s = 128$ for example 5.3

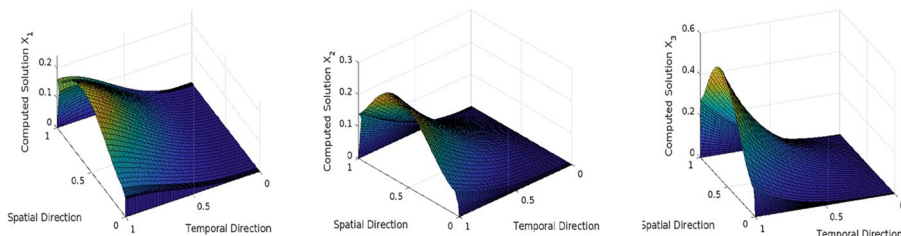


Fig. 12 When $\varepsilon_1 = 6^{-2}2^{-10}$, $\varepsilon_2 = 3^{-2}2^{-10}$, $\varepsilon_3 = 2^{-2}2^{-10}$, $\nu^2 = 4^{-2}2^{-10}$, $\mathcal{N}_x = \mathcal{N}_s = 128$ for example 5.3

6 Conclusions

In this work we have approximated efficiently the exact solution of a type of one-dimensional parabolic singularly perturbed systems for which the diffusion parameters are different at each equation of the system, but the convection parameter is the same for all equations. Moreover, in the partial differential equation associated to the continuous problem, a time delay term appears. In general, when the diffusion and the convection parameters take small values, the exact solution of the continuous problem has overlapping boundary layers at the end points, due to the different diffusion parameters, of the spatial domain; the width of the boundary layers depends on the value and the ratio between the diffusion and the convection parameters. To approximate numerically the exact solution of the continuous problem, we use a numerical method which combines the Crank-Nicolson method to discretize in time, constructed on a uniform mesh, and a cubic spline collocation method to discretize in space. Then, when the spatial discretization is constructed on and adequate non-uniform Shishkin mesh, the fully discrete scheme is a uniformly convergent method, having second order in time and almost second order in space. To see in practice the efficiency and the uniform convergence of the numerical algorithm, the numerical results obtained for some test problems are showed. These examples show that same technique, can be extended to systems with a larger number of equations. In the future, we will try extend similar ideas to the most interesting case of parabolic multidimensional singularly perturbed systems, again with small parameters in both the diffusion and the convection terms.

Table 8 For example 5.3 maximum point-wise errors and orders of convergence when $\alpha \cdot \nu^2 \leq \eta \cdot \varepsilon_1$.

δ	$\mathcal{N}_s = \mathcal{N}_x = 32$	$\mathcal{N}_s = \mathcal{N}_x = 64$	$\mathcal{N}_s = \mathcal{N}_x = 128$	$\mathcal{N}_s = \mathcal{N}_x = 256$	$\mathcal{N}_s = \mathcal{N}_x = 512$
2^0	$1.4686E-3$	$4.1960E-4$	$1.1656E-4$	$3.0674E-5$	$7.8651E-6$
2^{-2}	$3.8917E-3$	$1.1467E-3$	$3.0092E-4$	$8.1558E-5$	$2.0912E-5$
2^{-4}	$6.5384E-3$	$1.8162E-3$	$4.9086E-4$	$1.2917E-4$	$3.3121E-5$
2^{-6}	$9.4396E-3$	$2.7413E-3$	$7.6147E-4$	$2.0580E-4$	$5.2769E-5$
2^{-8}	$1.8359E-2$	$5.2175E-3$	$1.4154E-3$	$3.7247E-4$	$9.5505E-5$
2^{-10}	$2.4137E-2$	$6.9270E-3$	$1.9235E-3$	$5.1986E-4$	$1.3830E-4$
2^{-12}	$2.9745E-2$	$8.3820E-3$	$2.3245E-3$	$6.1171E-4$	$1.5685E-4$
2^{-14}	$3.0942E-2$	$8.6351E-3$	$2.3358E-3$	$6.1468E-4$	$1.5761E-4$
2^{-16}	$3.0986E-2$	$8.6388E-3$	$2.3392E-3$	$6.1489E-4$	$1.5795E-4$
2^{-18}	$3.0989E-2$	$8.6391E-3$	$2.3394E-3$	$6.1491E-4$	$1.5797E-4$
2^{-20}	$3.0990E-2$	$8.6392E-3$	$2.3394E-3$	$6.1493E-4$	$1.5798E-4$
2^{-22}	$3.0990E-2$	$8.6392E-3$	$2.3394E-3$	$6.1493E-4$	$1.5798E-4$
$E_1^{\mathcal{N}_s, \mathcal{N}_x}$	$3.0990E-2$	$8.6392E-3$	$2.3394E-3$	$6.1493E-4$	$1.5798E-4$
$R_1^{\mathcal{N}_s, \mathcal{N}_x}$	1.8428	1.8848	1.9276	1.9607	
CPU time (seconds)	1.0843	1.3285	1.4573	1.9538	2.1205

Table 9 For example 5.3 maximum point-wise errors and orders of convergence when $\alpha, \nu^2 \geq \eta, \varepsilon_3$.

δ	$\mathcal{N}_s = \mathcal{N}_x = 32$	$\mathcal{N}_s = \mathcal{N}_x = 64$	$\mathcal{N}_s = \mathcal{N}_x = 128$	$\mathcal{N}_s = \mathcal{N}_x = 256$	$\mathcal{N}_s = \mathcal{N}_x = 512$
2^0	$1.3133E-2$	$3.8253E-3$	$1.0213E-3$	$2.8170E-4$	$7.2232E-5$
2^{-2}	$2.1042E-2$	$6.0728E-3$	$1.6935E-3$	$4.5770E-4$	$1.2045E-4$
2^{-4}	$3.6420E-2$	$1.0465E-2$	$2.9322E-3$	$7.9249E-4$	$2.0320E-4$
2^{-6}	$4.2915E-2$	$1.2317E-2$	$3.4132E-3$	$9.2249E-4$	$2.3653E-4$
2^{-8}	$5.3572E-2$	$1.5328E-2$	$4.3521E-3$	$1.2252E-3$	$3.2242E-4$
2^{-10}	$6.5391E-2$	$1.8708E-2$	$5.2105E-3$	$1.4018E-3$	$3.6410E-4$
2^{-12}	$7.1982E-2$	$2.0217E-2$	$5.5102E-3$	$1.5220E-3$	$3.9635E-4$
2^{-14}	$7.8957E-2$	$2.2635E-2$	$6.3042E-3$	$1.7208E-3$	$4.5284E-4$
2^{-16}	$8.0919E-2$	$2.3150E-2$	$6.4134E-3$	$1.7054E-3$	$4.5879E-4$
2^{-18}	$8.1028E-2$	$2.3207E-2$	$6.4204E-3$	$1.7082E-3$	$4.5893E-4$
2^{-20}	$8.1030E-2$	$2.3208E-2$	$6.4206E-3$	$1.7083E-3$	$4.5894E-4$
2^{-22}	$8.1030E-2$	$2.3208E-2$	$6.4206E-3$	$1.7083E-3$	$4.5894E-4$
$E_1^{\mathcal{N}_s, \mathcal{N}_x}$	$8.1030E-2$	$2.3208E-2$	$6.4206E-3$	$1.7083E-3$	$4.5894E-4$
$R_1^{\mathcal{N}_s, \mathcal{N}_x}$	1.8038	1.8538	1.9101	1.8962	
CPU time (seconds)	1.1235	1.5231	1.6578	1.8532	1.9503

Table 10 For example 5.3 maximum point-wise errors and orders of convergence when $\eta \varepsilon_2 < \alpha \nu^2 < \eta \varepsilon_3$.

δ	$\varepsilon_1 = 8^{-2}\delta, \varepsilon_2 = 6^{-2}\delta, \varepsilon_3 = 2^{-2}\delta, \nu^2 = 4^{-2}\delta$	$\mathcal{N}_s = \mathcal{N}_x = 32$	$\mathcal{N}_s = \mathcal{N}_x = 64$	$\mathcal{N}_s = \mathcal{N}_x = 128$	$\mathcal{N}_s = \mathcal{N}_x = 256$	$\mathcal{N}_s = \mathcal{N}_x = 512$
2 ⁰	7.3911E-3	2.1951E-3	6.0975E-4	1.6217E-4	4.2122E-5	
2 ⁻²	2.6107E-2	7.2152E-3	1.9524E-4	5.0450E-5	1.2936E-5	
2 ⁻⁴	3.8526E-2	1.1058E-2	3.1359E-3	8.3848E-4	2.1666E-4	
2 ⁻⁶	5.0271E-2	1.4328E-2	3.9800E-3	1.0757E-3	2.7940E-4	
2 ⁻⁸	6.2851E-2	1.8075E-2	5.1208E-3	1.4041E-3	3.6470E-4	
2 ⁻¹⁰	7.0752E-2	2.0256E-2	5.6135E-3	1.5208E-3	4.0021E-4	
2 ⁻¹²	7.8537E-2	2.2453E-2	6.2145E-3	1.7208E-3	4.4696E-4	
2 ⁻¹⁴	8.0578E-2	2.3048E-2	6.4527E-3	1.7713E-3	4.5889E-4	
2 ⁻¹⁶	8.0652E-2	2.3108E-2	6.4602E-3	1.7795E-3	4.5902E-4	
2 ⁻¹⁸	8.0655E-2	2.3201E-2	6.4604E-3	1.7798E-3	4.5904E-4	
2 ⁻²⁰	8.0657E-2	2.3202E-2	6.4605E-3	1.7798E-3	4.5904E-4	
2 ⁻²²	8.0657E-2	2.3202E-2	6.4605E-3	1.7798E-3	4.5904E-4	
$E_1^{\mathcal{N}_s, \mathcal{N}_x}$	8.0657E-2	2.3202E-2	6.4605E-3	1.7798E-3	4.5904E-4	
$R_1^{\mathcal{N}_s, \mathcal{N}_x}$	1.7976	1.8445	1.8599	1.9550		
CPU time (seconds)	1.0945	1.1252	1.4825	1.6548	1.8235	

Table 11 For example 5.3 maximum point-wise errors and orders of convergence when $\eta \varepsilon_1 < \alpha \nu^2 < \eta \varepsilon_2$.

δ	$\varepsilon_1 = 6^{-2}\delta, \varepsilon_2 = 3^{-2}\delta, \varepsilon_3 = 2^{-2}\delta, \nu^2 = 4^{-2}\delta$	$\mathcal{N}_s = \mathcal{N}_x = 32$	$\mathcal{N}_s = \mathcal{N}_x = 64$	$\mathcal{N}_s = \mathcal{N}_x = 128$	$\mathcal{N}_s = \mathcal{N}_x = 256$	$\mathcal{N}_s = \mathcal{N}_x = 512$
2^0	1.7937E-2	5.1352E-3	1.4250E-3	3.8514E-4	1.0004E-4	1.0004E-4
2^{-2}	2.4514E-2	6.9137E-3	1.9185E-3	5.0754E-4	1.3014E-4	1.3014E-4
2^{-4}	3.7937E-2	1.0924E-2	3.0315E-3	8.0198E-4	2.0564E-4	2.0564E-4
2^{-6}	4.5572E-2	1.3056E-2	3.6312E-3	9.7091E-4	2.5088E-4	2.5088E-4
2^{-8}	5.1851E-2	1.4852E-2	4.1460E-3	1.1052E-3	2.8338E-4	2.8338E-4
2^{-10}	6.2753E-2	1.7935E-2	4.9736E-3	1.4508E-3	3.7781E-4	3.7781E-4
2^{-12}	6.8732E-2	1.9657E-2	5.4129E-3	1.4588E-3	3.7805E-4	3.7805E-4
2^{-14}	7.5628E-2	2.1678E-2	6.0343E-3	1.6253E-3	4.1781E-4	4.1781E-4
2^{-16}	7.8925E-2	2.2517E-2	6.3142E-3	1.7105E-3	4.3972E-4	4.3972E-4
2^{-18}	7.8929E-2	2.2519E-2	6.3145E-3	1.7108E-3	4.3974E-4	4.3974E-4
2^{-20}	7.8929E-2	2.2519E-2	6.3145E-3	1.7108E-3	4.3974E-4	4.3974E-4
2^{-22}	7.8929E-2	2.2519E-2	6.3145E-3	1.7108E-3	4.3974E-4	4.3974E-4
$E_1^{\mathcal{N}_s, \mathcal{N}_x}$	7.8929E-2	2.2519E-2	6.3145E-3	1.7108E-3	4.3974E-4	4.3974E-4
$R_1^{\mathcal{N}_s, \mathcal{N}_x}$	1.8094	1.8344	1.8840	1.9599		
CPU time (seconds)	1.1072	1.1247	1.3809	1.4572	1.6827	

Funding Open Access funding provided thanks to the CRUE-CSIC agreement with Springer Nature. The research of second author was partially supported by the project PID2022-136441NB-I00, the Aragón Government and the European Social Fund (group E24-17R).

Declarations

Competing interests The authors claim that, to the best of their knowledge, their assertions are uninfluenced by competing interests.

Open Access This article is licensed under a Creative Commons Attribution 4.0 International License, which permits use, sharing, adaptation, distribution and reproduction in any medium or format, as long as you give appropriate credit to the original author(s) and the source, provide a link to the Creative Commons licence, and indicate if changes were made. The images or other third party material in this article are included in the article's Creative Commons licence, unless indicated otherwise in a credit line to the material. If material is not included in the article's Creative Commons licence and your intended use is not permitted by statutory regulation or exceeds the permitted use, you will need to obtain permission directly from the copyright holder. To view a copy of this licence, visit <http://creativecommons.org/licenses/by/4.0/>.

References

1. Amrein, M., Wihler, T.P.: Fully adaptive Newton-Galerkin time stepping methods for singularly perturbed parabolic evolution equations. <https://arxiv.org/abs/1510.00622> (2015)
2. Avijit, D., Natesan, S.: SDFEM for singularly perturbed boundary-value problems with two parameters. *J. Appl. Math. Comput.* **64**, 591–614 (2020)
3. Bansal, K., Sharma, K.K.: Parameter-robust numerical scheme for time-dependent singularly perturbed reaction–diffusion problem with large delay. *Appl. Math. Comput.* **337**, 417–429 (2018)
4. Cengizci, S., Srinivasan, N., Atay, M.T.: A hybrid simulation for a system of singularly perturbed two-point reaction-diffusion equations, arXiv Preprint <https://arxiv.org/abs/1710.01694> (2017)
5. Clavero, C., Gracia, J.L., Jorge, J.C.: High-order numerical methods for one dimensional parabolic singularly perturbed problems with regular layers. *Num. Meth. Part. Diff. Equ.* **21**, 149–169 (2005)
6. Clavero, C., Jorge, J.C.: A splitting uniformly convergent method for one-dimensional parabolic singularly perturbed convection-diffusion systems. *Appl. Num. Meth.* **183**, 317–332 (2023)
7. Clavero, C., Kumar, S., Kumar, S.: A priori and a posteriori error estimates for efficient numerical schemes for coupled systems of linear and nonlinear singularly perturbed initial-value problems. *Appl. Num. Meth.* **208**, 123–147 (2025)
8. Clavero, C., Shiromani, R., Shanthi, V.: A numerical approach for a two-parameter singularly perturbed weakly-coupled system of 2-D elliptic convection-reaction-diffusion pde. *J. Comput. Appl. Math.* **436**, 115422 (2024). <https://doi.org/10.1016/j.cam.2023.115422>
9. Clavero, C., Shiromani, R., Shanthi, V.: A computational approach for 2D elliptic singularly perturbed weakly-coupled systems of convection-diffusion type with multiple scales and parameters in the diffusion and the convection terms. *Math. Meth. Appl. Sci.* **47**, 13510–13541 (2024). <https://doi.org/10.1002/mma.10204>
10. Clavero, C., Shiromani, R.: An efficient numerical method for 2D elliptic singularly perturbed systems with different magnitude parameters in the diffusion and the convection term. *Comput. Math. Appl.* **181**, 287–322 (2025). <https://doi.org/10.1016/j.camwa.2025.01.011>
11. Ghil, M., Robertson, A.W.: Climate dynamics and predictability. *Bull. Am. Meteorolog. Soc.* **83**, 571–591 (2002)
12. Govindarao, L., Mohapatra, J., Sahu, S.R.: Uniformly convergent numerical method for singularly perturbed two parameter time delay parabolic problem. *Int. J. Appl. Comput. Math.* **5** (2019). <https://doi.org/10.1007/s40819-019-0672-5>
13. Hall C.A., On error bounds for spline interpolation. *J. Appr. Theo.* **1**, 209–218 (1968)
14. Kadalbajoo, M.K., Patidar, K.C.: A survey of numerical techniques for solving singularly perturbed delay differential equations. *Appl. Math. Comput.* **134**, 371–429 (2003)

15. Kumar, D., Kumari, P.: Fitted mesh B-spline collocation method for singularly perturbed differential-difference equations with small delay. *J. Comput. Appl. Math.* **339**, 1–15 (2018)
16. Kumar, D.: A uniformly convergent scheme for two-parameter problems having layer behaviour, *inter. J. Comput. Math.* **99**(3), 553–574 (2021)
17. Kumar, S., Kumar, M.: An efficient hybrid numerical method based on an additive scheme for solving coupled systems of singularly perturbed linear parabolic problems. *Math. Meth. Appl. Scie.* **46**, 1234–1256 (2023)
18. Kumari, N., Gowrisankar, S.: A robust B-spline method for two parameter singularly perturbed parabolic differential equations with discontinuous initial condition. *J. Appl. Math. Comput.* **70**, 5379–5403 (2024)
19. Kumari, P., Singh, S., Kumar, D.: An effective numerical approach for solving a system of singularly perturbed differential-difference equations in biology and physiology. *Math. Comput. Simul.* **229**, 553–573 (2025)
20. Kumari, P., Clavero, C.: Spline-based approximation for two-parameter singularly perturbed systems with large time delay with applications in science and engineering. *Math. Comput. Simul.* **241**, 326–350 (2026). <https://doi.org/10.1016/j.matcom.2025.09.001>
21. Ladyženskaja, O.A., Solonnikov, V.A., Ural'tseva, N.N.: Linear and quasilinear equations of parabolic type, translated from the Russian by S. Smith. *Translations Math. Monogr. Am. Math. Soc.*, Providence **23** (1968)
22. L. Mehdi Lotfi, E., Radouane, Y., Noura, Y.: A generalized reaction-diffusion epidemic model with time delay, *discont. Nonli. Compl.* **3**(1), 1–6 (2014)
23. Miller, J.J.H., O'Riordan, E., Shishkin, G.I.: *Fitted Numerical Methods for Singular Perturbation Problems: error Estimates in the Maximum Norm*. World Scientific, Singapore (2012)
24. Mohanty, R.K., Jha, P.K.: A cubic spline collocation method for singularly perturbed delay differential equations. *Numer. Meth. Part. Diff. Equ.* **35**, 2198–2217 (2019)
25. Murray, J.D.: *Mathematical Biology I: An Introduction*. Springer (2002)
26. O'Riordan, E., Pickett, M.L., Shishkin, G.I.: Parameter-uniform finite difference schemes for singularly perturbed parabolic diffusion-convection-reaction problems. *Math. Comput.* **75**, 1135–1154 (2006)
27. Singh, S., Kumari, P., Kumarr, D.: An effective numerical approach for two parameter time-delayed singularly perturbed problems. *Comput. Appl. Math.* **41** (2022). <https://doi.org/10.1007/s40314-022-02046-3>
28. Sharma, K.K., Sharma, N.: Fitted mesh method for solving singularly perturbed delay differential equations. *Int. J. Comput. Math.* **93**, 829–842 (2016)
29. Singh, S., Kumar, D.: Parameter uniform numerical method for a system of singularly perturbed parabolic convection-diffusion equations. *Math. Comput. Simul.* **212**, 360–381 (2023)
30. Varah, J.M.: A lower bound for the smallest singular value of a matrix, *Lin. Alg. Appl.* **11**, 3–5 (1975)
31. Woldaregay, M.A.: Novel numerical scheme for singularly perturbed time delay convection-diffusion equation. *Adv. Math. Phys.* **2021**, Article ID 6641236 (2021)

Publisher's Note Springer Nature remains neutral with regard to jurisdictional claims in published maps and institutional affiliations.

Authors and Affiliations

Parvin Kumari¹ · Carmelo Clavero² 

 Carmelo Clavero
clavero@unizar.es

Parvin Kumari
parvin.kumari@jaipur.manipal.edu

¹ Manipal University Jaipur, Jaipur, India

² Department of Applied Mathematic and IUMA, University of Zaragoza, Zaragoza, Spain